USING INVERSE EULER EQUATIONS TO SOLVE MULTIDIMENSIONAL DISCRETE-CONTINUOUS DYNAMIC MODELS: A GENERAL METHOD

LORETTI I. DOBRESCU* AND AKSHAY SHANKER†

ABSTRACT. We develop a general inverse Euler equation method to efficiently solve any multidimensional stochastic dynamic optimization problem with agents facing discrete-continuous choices and occasionally binding constraints. First, we provide a discrete time analogue to the Hamiltonian to (painlessly) recover the generalized necessary Euler equation. We then establish necessary and sufficient conditions to determine the existence of an Euler equation inverse, and the structure of the exogenous computational grid on which the inverse is well-defined. To handle applications with non-convexities generated by discrete choices, we finally present an off-the-shelf 'rooftop-cut' algorithm guaranteed to asymptotically recover the optimal policy function under standard economic assumptions. We demonstrate our approach using two workhorse applications in the literature, and document the computational speed and accuracy gains our method generates.

Key Words: discrete and continuous choices, non-convex optimization, Euler equation, dynamic programming, inverse optimization

JEL Classification: C13, C63, D91

* Corresponding author. School of Economics, University of New South Wales, Sydney 2052 Australia. Email: dobrescu@unsw.edu.au.

† School of Economics, University of New South Wales, Australia and ARC Center for Excellence in Population Ageing Research (CEPAR), Sydney 2052 Australia. Email: a.shanker@unsw.edu.au.

‡ We thank Max Blesch, Chris Carroll, Mateo Velasquez-Giraldo, Greg Kaplan, Sebastian Gsell, Mike Keane, Anant Mathur, Olivia Mitchell, Adrian Monninger, Lucas Pahl, and John Stachurski for valuable discussions and comments. Research support from the Australian Research Council (ARC LP150100608) and ARC Centre of Excellence in Population Ageing Research (CE17010005) is gratefully acknowledged. This research was undertaken with the assistance of resources and services from the National Computational Infrastructure (NCI), which is supported by the Australian Government. The software implementing the RFC algorithm and the applications can be found here.

1. Introduction

The prolonged focus on consumption and saving behavior, economic mobility, income and wealth inequality, social insurance, and redistributive policies has led economists to increasingly incorporate agent heterogeneity and behavioral frictions into dynamic decision-making models with uncertainty. Such models have been widely employed to help us understand, for instance (i) life-cycle wealth accumulation (French, 2005; Fagereng et al., 2017; Dobrescu et al., 2018), (ii) saving frictions (Kaplan and Violante, 2014; Berger and Vavra, 2015; Kaplan et al., 2020), (iii) labour choices (Attanasio et al., 2018; Iskhakov and Keane, 2021), (iv) housing dynamics (Cocco, 2005; Yogo, 2016; Fagereng et al., 2019) and mortgage refinancing effects on life-cycle asset allocation (Laibson et al., 2021), (v) risk of defaulting (Arellano, 2008; Arellano et al., 2016; Jang and Lee, 2023), (vi) firm investments with adjustment costs (Cooper, 2006; Khan and Thomas, 2008; Alfaro et al., 2024), as well as (vii) precautionary savings motives (Aiyagari, 1994; Carroll, 1997; Gourinchas and Parker, 2002), (viii) wealth accumulation with liquidity constraints (Deaton, 1991; Carroll, 1997; Dávila et al., 2012), (xi) distributional effects of business cycles (Krusell and Smith, 1998; Buera and Moll, 2015), and (x) policy transmission (Krueger et al., 2016; Kaplan et al., 2018; Beraja and Zorzi, 2023).

The challenges associated with solving and estimating these models are well known. Due to the curse of dimensionality (Rust, 1987), doing so is highly prohibitive using standard numerical methods. Even with the recent advances in computing power, applying the most novel computational methods proposed in the last few years (e.g., adaptive sparse grids - Brumm and Scheidegger (2017), polynomial chaos expansions - Pröhl (2023), machine learning - Duarte et al. (2020); Fernández-Villaverde et al. (2023)) to more interesting versions of these models remains a complex and computationally highly intensive endeavor. Several studies have recognized that significant speed and accuracy can be gained in standard settings by solving the Euler equation of the multidimensional dynamic stochastic optimization problem (Coleman, 1990; Reffett, 1996; Li and Stachurski, 2014). Additionally, methods that involve inverting Euler equations (e.g., endogenous grid method, EGM)[1] were even shown to eliminate the need for numerical methods altogether (Carroll, 2006).

However, studies (i)-(vi) above prominently feature discrete choices, while occasionally binding constraints (such as liquidity constraints) are central in studies (vii)-(x). These elements lead to a breakdown of the standard convexity and smoothness assumptions required for Euler equation methods to work in a transparent and robust manner (Achdou et al., 2021). First, discrete choices introduce non-concavity of the value function, which can lead to multiple sub-optimal solutions to the Euler equation (Iskhakov et al., 2017). Second, with both discrete choices and occasionally binding constraints, policy functions may not be differentiable everywhere, precluding the

[1]Other methods that use Euler equations include Coleman-Reffett policy iteration (Coleman, 1990; Reffett, 1996; Li and Stachurski, 2014), the envelope condition method (Maliar and Maliar, 2013; Arellano et al., 2016), and deep learning methods that minimize the Euler equation error (Maliar et al., 2021).

use of standard envelope condition methods to derive the Euler equation (González-Sánchez and Hernández-Lerma, 2013). One must thus employ restrictive assumptions (i.e., boundedness, compactness) on the reward functions and feasibility correspondences (Rincón-Zapatero and Santos, 2009; Rendahl, 2015) that are generally violated in less stylized settings (Carroll, 2023). Third, when using methods that invert the Euler equation to reduce the numerical burden involved in solving multidimensional models, one does not know what conditions (that can be easily verified) are required for the inverse to be well-defined. Additionally, when occasionally binding constrains are also involved, there are no results to determine the optimal constraint choice implied by an inverse solution without going back to costly numerical optimization (Druedahl and Jørgensen, 2017). Finally, there are no results in general addressing any of these challenges for discrete time applications. Hence, applying Euler equation methods in dynamic stochastic modelling, while promising, has so far been stylized or ad hoc, and often incorporated alongside costly numerical optimization in more complex problems.

Our paper aims to close this gap. In particular, using recent advances in inverse optimization (Iyengar and Kang, 2005; Chan et al., 2023),[2] we develop a general inverse Euler equation method to solve dynamic stochastic optimization problems that resolves all the challenges above. To achieve this, we derive a generalized necessary Euler equation, characterize its invertibility, and provide an efficient algorithm to recover the optimal policy function in the presence of multiple local optima.

In doing so, we see our contribution as threefold. First, as mentioned, we formalize the necessary recursive Euler equation, doing so for any *any* multidimensional dynamic stochastic optimization problems, including those with agents facing discrete choices and occasionally binding constraints. The approach we take is to characterize the Euler equation by introducing a discrete time analogue to the stochastic Hamiltonian - the 'S-function'. The S-function represents the change in the objective function value given a time-, state- and information-specific perturbation of the current period state. The S-function differentiation can then be defined in terms of real-valued calculus on the model primitives, and the Euler equation can be recovered without cumbersome envelope conditions or abstract functional derivatives. This is extremely beneficial in less stylized applications.

Second, we give necessary and sufficient conditions for the Euler equation invertibility that can robustly handle occasionally binding constraints. Recall that methods that invert the Euler equation reduce the need to find numerical solutions to dynamic optimization problems (Iyengar and Kang, 2005; Carroll, 2006). Our innovation is to define the inverse Euler equation on the joint space of end-of-period states (or 'post-states') *and* intratemporal Kuhn-Tucker multipliers of the constraints (i.e., the space of 'observable variables'), which allows us to robustly handle occasionally binding constraints. We then provide necessary and sufficient conditions for 'pure EGM',

[2]Inverse optimization is founded in geophysics (Sen and Stoffa, 2013) and has more recently gained tremendous traction in the AI literature, where inverse reinforcement learning has been used to recover parameters from observed actions. Up to our best knowledge, we are the first to formalise and deploy this theory as a formal method to solve dynamic stochastic optimization problems.

a situation where the Euler equation can always be inverted (analytically or numerically) on the space of observable variables. One fundamental insight of the results here is that the structure of the exogenous grid on which the inverse Euler equation is well-defined is solely determined by the state space dimension, even in regions where constraints bind. To use pure EGM, the number of post-states must be equal to the state space dimension, allowing us to formally define an inverse Euler equation that maps directly to the first order conditions (FOCs) of the S-function, and thus clearly identifies which constraints bind in each region of the exogenous grid.

Obviously, in applications with more post-states than states, pure EGM cannot be applied (e.g., Berger and Vavra (2015); Kaplan et al. (2020)). For such situations, we provide the conditions on the policy function (i.e., local injectivity and continuity) guaranteeing that the Euler equation can be inverted from a reduced-dimensional subset (i.e., submanifold) of the observable space. Numerical root-finding can then be used to construct the exogenous grid such that our inverse Euler equation method can still bring significant computational efficiency gains. Note also that these results allow the inverse Euler equation to be robustly employed in any model (with or without discrete choices) where an analytical inverse to the Euler equation may not exist.

Third, we present a computationally efficient, accurate, and user-friendly algorithm to obtain the optimal policy functions for any multidimensional dynamic stochastic optimization problem with both discrete and continuous choices and occasional binding constraints. The algorithm, dubbed 'rooftop-cut' (or RFC), checks each solution point (i.e., each point of the endogenous grid) to see if the tangent to the future choice-specific value function at that point dominates neighboring points. If a neighboring point is dominated and moving to it induces a jump in the policy function, then this point is removed as sub-optimal. If a neighboring point dominates the tangent, it is retained in the endogenous (solution) grid. Note here that RFC has the advantage of being able to recover the upper envelope of the value correspondence generated by the local solutions to the necessary Euler equation regardless of the interpolation method on the irregular multidimensional endogenous grid. It can also be easily programmed using vectorized (array) operations, making it compatible with high-performance computing infrastructure and programming languages.

Fourth, we provide pointwise asymptotic error bounds for our inverse Euler equation method both in the discrete-continuous case and for applications without discrete choices. We do so under standard economic assumptions that only relate to the Lipshitz continuity of the policy function (White, 2015). This is particularly useful in simulation-based studies where the moments generated by the optimal policies computed via generalized inverse Euler equation and RFC (or EGM without discrete choices) become asymptotically accurate as the exogenous grid is refined.

Finally, we present two widely-used applications to illustrate the applicability of our method. Consider first a life-cycle model a' la Druedahl and Jørgensen (2017) in which agents facing unemployment risks decide how much to save in pensions and financial assets, and whether to retire or not. In this case, we show how the Euler

equation derived using the S-function can be used to determine the optimal binding constraints given a point in the exogenous grid, without deriving separate policy functions for each constrained choice and without numerical loops to optimize over the constraint choices. With four possible combinations of binding constraints, RFC with Delaunay triangulation is (i) as fast as the original method by Druedahl and Jørgensen (2017), both methods being two orders of magnitude faster than value function iteration (VFI), and (ii) slightly more accurate, with gains coming from using first order information to 'delete' sub-optimal points. Adding just one extra single constraint (e.g., a cap on pension contributions) leads to 50% increase in the number of possible binding constraint combinations, and so 50% increase in the computation time using the original method. On the other hand, using our inversion results to determine the optimal constraint from the exogenous grid and RFC leaves total computation time unchanged. Next, we do the same to examine a portfolio allocation problem with housing and financial assets, where previous discrete-continuous Euler equation methods fail due to (i) non-monotonic policy functions, and (ii) an irregular exogenous grid that arises because the Euler equation is not analytically invertible. Somewhat unsurprisingly, we find RFC to be again two orders of magnitude faster and more accurate than standard VFI. Compared, however, to the most efficient prior attempts to solve this type of problems, which use an EGM step nested within numerical optimization (Druedahl, 2021), RFC gains up to an order of magnitude better accuracy and 25% higher speed.

Our paper advances considerably the latest dynamic programming methods. First, in relation to the theoretical foundation of Euler equations (Sorger, 2015; Rincón-Zapatero and Santos, 2009; Li and Stachurski, 2014; Rendahl, 2015; Ma et al., 2022; Stachurski, 2022), we are the first to provide the necessary and sufficient conditions for the generalized Euler equation to accommodate occasionally binding constraints, discrete choices, unbounded rewards, and non-compact feasibility correspondences. Second, while the underlying intuition behind inverting the Euler equation and EGM as an inverse problem was introduced in a special case by Carroll (2006) and has spawned a significant literature (Barillas and Fernandez-Villaverde, 2007; White, 2015; Iskhakov, 2015; Ludwig and Schön, 2018; Lujan, 2023), we are the first to develop a formal theory of inverse optimization to solve discrete-continuous dynamic stochastic problems even when facing the challenges detailed above. Specifically, we provide (i) verifiable error bounds, (ii) necessary and sufficient conditions for EGM to be well-defined (with or without discrete choices), and (iii) the conditions that characterize the structure of the exogenous grids. Third, in terms of the EGM implementation in discrete-continuous choice models (Fella, 2014; Iskhakov et al., 2017; Druedahl and Jørgensen, 2017; Druedahl, 2021), our RFC algorithm is the first to (i) not require regularity of the exogenous grid or monotonicity of the optimal policy, (ii) be asymptotically guaranteed to approximate the optimal solution, and (iii) allow high-dimensional discrete-continuous models to exploit the massive parallelism of modern high performance computing infrastructure (e.g., GPUs). Up to our best knowledge, only Dobrescu and Shanker (2023) attempts to recover the upper envelope of the value correspondence for discrete-continuous EGM when the policy function is

non-monotone. Unlike RFC, which works in multiple dimensions and uses the value function gradient, the FUES method by Dobrescu and Shanker (2023) (i) uses secants to eliminate neighboring points, (ii) can only be applied to one-dimensional problems, and importantly, (iii) does not address any of the theoretical challenges listed above. Finally, our paper relates to the broader optimization literature that seeks to address the issues associated with numerically solving richer, more complex dynamic models. For instance, Brumm and Scheidegger (2017) tackles the high-dimensionality of their model by developing a method to refine sparse grids, Achdou et al. (2021) suggests continuous time modelling, and Maliar et al. (2021) and Auclert et al. (2021) propose ways to arrive at and approximate the stationary policies. Our work complements these approaches by developing a method that focuses on the within period solution in (stationary or non-stationary) discrete time models. Moreover, it can accurately handle non-convexities arising from discrete choices, and also allows models to efficiently scale with the dimension of the state and the number of constraint choices. This makes it applicable to all multidimensional dynamic stochastic optimization problems in which non-smooth, non-monotone and discontinuous policy functions lead to computational challenges. Consequently, while our results support a more direct implementation of Euler equation methods in stylized applications (Aiyagari, 1994; Huggett, 1996; Krusell and Smith, 1998; Fella, 2014; Iskhakov et al., 2017; Druedahl and Jørgensen, 2017), they also allow more interesting, complex multidimensional models – such as heterogeneous agents models with household formation and labour choices (Kekre, 2022; Bardoćzy, 2022), structural life-cycle models with consumer credit (Best et al., 2019; Crawford and O'Dea, 2020; Dobrescu et al., 2024b) or dynamic human capital accumulation (Hai and Heckman, 2019; Dobrescu et al., 2024a) – to be solved and estimated efficiently.

The paper proceeds as follows. Section 2 introduces the setup of a general dynamic programming problem, and discusses the challenges to the Euler equation identified in the literature. Section 3 introduces the S-function and proves the necessary FOCs. Section 4 formalizes the inverse dynamic optimization problem, provides necessary and sufficient conditions for the invertibility of the Euler equations, and introduces the RFC algorithm with its convergence properties. Section 5 presents two applications of the theory, together with the analysis of the accuracy and speed gains from our method compared to previous ones. Section 6 concludes.

2. General setup and preliminary considerations

In what follows, we use italic to denote variables, roman fonts for functions, and capital letters for spaces - e.g., at time t, y_t is a variable in the post-decision state (or 'post-state') space Y_t, with $y_t \in Y_t$, and y_t is the post-state policy function.[3] Additionally, we use (i) bold letters with a $\vec{\ }$ superscript to denote a sequence of

[3]To further streamline exposition, we will use italic to denote both (i) a random variable that realizes in the state and post-state space ('history contingent plans', see Hernandez-Lerma and Lasserre (2012)), and (ii) the realized value of a random variable, as a state or post-state, at a given time - a distinction that will become important when we prove our results in the appendix.

variables across time - e.g., $\vec{\boldsymbol{y}}_t = \{y_t, y_{t+1}, \ldots, y_T\}$, with T the terminal period of the dynamic programming problem, and (ii) capital calligraphic letters for a sequence of grid points labelled with superscript $^{\#}$ - e.g., $\mathcal{Y}_t = \left\{y^{\#}_{t,0}, \ldots, y^{\#}_{t,N}\right\}$ is a grid of N post-state points at time t, with $\mathcal{Y}_t \subset Y_t$. For completeness, we relegate the remaining standard notation to the online appendix D.1.

2.1. **General problem setup.** We start by setting up a general reduced form, non-stationary, discrete-continuous stochastic dynamic optimization problem consistent with recent literature (Hernandez-Lerma and Lasserre, 2012; Hull, 2015; Druedahl and Jørgensen, 2017; Ma et al., 2022; Sargent and Stachurski, 2023). Let t index time, and assume $t \in \{0, \ldots, T\}$, where $T \in \mathbb{N} \cup \{\infty\}$. The problem consists of a tuple $\{X_t, W_t, D_t, Y_t, \Gamma_t, \mathrm{u}_t, \mathrm{F}_t\}_{t=0}^{T}$, with

(1) State space $X_t = W_t \times Z_t \times M_t$ for each t, where
   (i) W_t is an exogenous shock space, with $W_t \subset \mathbb{R}^{N_W}$,
   (ii) Z_t is a finite discrete state space, with $Z_t \subset \mathbb{R}^{N_Z}$, and
   (iii) M_t is a compact and connected continuous state space, with $M_t \subset \mathbb{R}_+^{N_M}$.
(2) A W_t-valued sequence of shocks, $\{w_t\}_{t=0}^{T}$, with transition kernel F_t^w.[4]
(3) An action space $D_t \times Y_t$ for each t, where
   (i) D_t is a countable discrete choice space, with $D_t \subset \mathbb{N}^{N_D}$, and
   (ii) Y_t is a connected continuous post-state space, with $Y_t \subset \mathbb{R}^{N_Y}$.
(4) A feasibility correspondence Γ_t for each t, with $\Gamma_t \colon X_t \rightrightarrows D_t \times Y_t$, where $(d_t, y_t) \in \Gamma_t(x_t)$ if and only if $\mathrm{g}_t(w_t, z_t, m_t, d_t, y_t) \geq 0$ for g_t, where $\mathrm{g}_t(w_t, z_t, \cdot, d_t, \cdot) \colon \mathbb{R}^{N_M} \times \mathbb{R}^{N_Y} \to \mathbb{R}^{N_g}$ is continuously differentiable for each $(w_t, z_t, d_t) \in W_t \times Z_t \times D_t$.
(5) A concave reward function u_t for each t, with $\mathrm{u}_t \colon \mathrm{Gr}\Gamma_t \to \mathbb{R} \cup \{-\infty\}$.
(6) A transition kernel $\mathrm{F}_t \colon = (\mathrm{F}_t^w, \mathrm{F}_t^d, \mathrm{F}_t^m)$ for each t, where F_t^w is the shock transition defined above, F_t^d is the discrete state transition, with $\mathrm{F}_t^d \colon D_t \times W_{t+1} \to Z_{t+1}$, and F_t^m is the continuous state transition, with $\mathrm{F}_t^m \colon D_t \times Y_t \times W_{t+1} \to M_{t+1}$.

Each period, the agent observes a state x_t and responds with two state-contingent actions: a feasible discrete choice $d_t \in D_t$, and a continuous post-state $y_t \in Y_t$ such that $(d_t, y_t) \in \Gamma_t(x_t)$. The agent obtains a reward $\mathrm{u}_t(w_t, z_t, m_t, d_t, y_t)$ and randomly moves to the next period state x_{t+1}, with $x_{t+1} = (w_{t+1}, z_{t+1}, m_{t+1})$ and

$$x_{t+1} = \mathrm{F}_t(d_t, y_t, w_{t+1}). \tag{1}$$

Let v_0, with $\mathrm{v}_0 \colon X_0 \to \mathbb{R} \cup \{-\infty\}$, denote the initial period value function. The agent chooses measurable policy functions $\{\mathrm{d}_t, \mathrm{y}_t\}_{t=0}^{T}$, with $\mathrm{d}_t \colon X_t \to D_t$ and $\mathrm{y}_t \colon X_t \to Y_t$, to solve

$$(\mathbf{DP}) \qquad \mathrm{v}_0(x_0) \colon = \sup_{\{\mathrm{d}_t, \mathrm{y}_t\}_{t=0}^{T}} \mathbb{E}_{x_0}\left[\sum_{t=0}^{T} \mathrm{u}_t(w_t, z_t, m_t, \mathrm{d}_t(x_t), \mathrm{y}_t(x_t))\right], \qquad x_0 \in X_0,$$

[4]Without loss of generality, assume (i) $w_{t+1} = \mathrm{F}_t^w(w_t, \eta_{t+1})$ for a measurable F_t^w, where $\{\eta_t\}_{t=0}^{T}$ are random variables defined on a probability space $(\Omega, \Sigma, \mathbb{P})$, and (ii) w_0 is degenerate (Borovkov, 2013; Stachurski, 2022).

such that (1) holds with $y_t = \mathrm{y}_t(x_t)$, $d_t = \mathrm{d}_t(x_t)$ and $(\mathrm{d}_t(x_t), \mathrm{y}_t(x_t)) \in \Gamma_t(x_t)$ - i.e., the sequence $\{\mathrm{d}_t, \mathrm{y}_t\}_{t=0}^T$ is feasible. Since our aim is to provide a general method to characterize and solve (**DP**), we assume for brevity the existence of a recursive solution.

Assumption 2.1. *There exists policy functions* $\{\mathrm{d}_t, \mathrm{y}_t\}_{t=0}^T$ *such that the Bellman equation for* (**DP**) *satisfies*

(**BE**) $$\mathrm{v}_t(x_t) = \max_{d_t, y_t \in \Gamma_t(x_t)} \left[\mathrm{u}_t(w_t, z_t, m_t, d_t, y_t) + \mathbb{E}_{x_t} \mathrm{v}_{t+1}(x_{t+1})\right], \qquad x_t \in X_t, \forall t.$$

Choice-specific value functions. The current choice-specific value function is

(**CS-BE**) $$\mathrm{v}_{d_t,t}(x_t) := \max_{y_t \in \Gamma_{d_t,t}(x_t)} \left[\mathrm{u}_t(w_t, z_t, m_t, d_t, y_t) + \mathbb{E}_{x_t} \mathrm{v}_{t+1}(x_{t+1})\right], \qquad x_t \in X_t, \forall t,$$

where $\Gamma_{d_t,t}(x_t) := \{y_t \mid d_t, y_t \in \Gamma_t(x_t)\}$. Let $\mathrm{y}_{d_t,t}$ denote the current choice-specific (continuous state) policy function. (In applications, the objective is to approximate $\mathrm{v}_{d_t,t}$ and $\mathrm{y}_{d_t,t}$.) Next, fix x_t, let $\vec{\boldsymbol{d}}_t = \{d_t, \ldots, d_T\}$ be a stochastic sequence of *future discrete choices* starting at time t and ending at T,[5] and define the future choice-specific value function as

(**FS-DP**) $$\mathrm{v}_t^{\vec{\boldsymbol{d}}_t}(x_t) := \max_{\{\mathrm{y}_j\}_{j=t}^T} \mathbb{E}_{x_t}\left[\sum_{j=t}^{T} \mathrm{u}_j(w_j, z_j, m_j, d_j, \mathrm{y}_j(x_j))\right], \qquad x_t \in X_t \, \forall t,$$

such that $(d_t, \mathrm{y}_t(x_t)) \in \Gamma_t(x_t)$. Then, let $\vec{\boldsymbol{\Gamma}}_t(x_t)$ be the set of feasible future discrete choices starting at t, with $\vec{\boldsymbol{\Gamma}}_t(x_t) := \left\{\vec{\boldsymbol{d}}_t \in \bigtimes_{j=t}^T D_j \,\middle|\, d_j, y_j \in \Gamma_j\left(x_j\right), x_{j+1} = \mathrm{F}_j\left(d_j, y_j, w_{j+1}\right)\right\}$.[6] While it is computationally impractical to evaluate $\mathrm{v}_t^{\vec{\boldsymbol{d}}_t}(x_t)$ for each $\vec{\boldsymbol{d}}_t$, $\mathrm{v}_{d_t,t}$ incorporates the choice of $\vec{\boldsymbol{d}}_{t+1}$, and

$$\mathrm{v}_{d_t,t}(x_t) = \max_{y_t \in \Gamma_{d_t}(x_t)} \max_{\vec{\boldsymbol{d}}_{t+1} \in \vec{\boldsymbol{\Gamma}}_{t+1}(x_{t+1})} \Big\{ \underbrace{\mathrm{u}_t(w_t, z_t, m_t, d_t, y_t) + \mathbb{E}_{x_t} \mathrm{v}_{t+1}^{\vec{\boldsymbol{d}}_{t+1}}(w_{t+1}, z_{t+1}, m_{t+1})}_{=: \mathrm{Q}_t^{\vec{\boldsymbol{d}}_{t+1}}(x_t, d_t, y_t)} \Big\},$$

such that (1) holds. Finally, define the continuation value Q_t as

(**Q**) $$\mathrm{Q}_t(x_t, d_t, y_t) := \max_{\vec{\boldsymbol{d}}_{t+1}} \mathrm{Q}_t^{\vec{\boldsymbol{d}}_{t+1}}(x_t, d_t, y_t).$$

Generalized Euler equation and the inverse problem. We start by noting that current choice-specific policy functions $\mathrm{y}_{d_t,t}$ are approximated given a tuple of start-of-period fixed variables ξ_t, where $\xi_t := (w_t, z_t, d_t)$.

Definition 1. *Fix* t *and* ξ_t. *The function* $\mathbf{E}_t$, *with* $\mathbf{E}_t : Y_t \times \mathbb{R}_+^{N_g} \times M_t \to \mathbb{R}^{N_Y} \times \mathbb{R}^{N_g}$, *is a generalized Euler equation if, for each* $m_t \in M_t$, *there exists a multiplier* $\mu_t \in \mathbb{R}_+^{N_g}$ *such that* $\mathbf{E}_t(y_t, \mu_t, m_t) = 0$ *for feasible* y_t *if and only if* y_t *solves* (**CS-BE**) *given* ξ_t.

[5] The sequence $\{d_j, x_j\}_{j=t}^T$ can be *generated* by $\{\mathrm{d}_j, \mathrm{y}_j\}_{j=t}^T$ using $d_j = \mathrm{d}_j(x_j)$ and $x_{j+1} = \mathrm{F}(d_j, \mathrm{y}_j(x_j), w_{j+1})$.

[6] $\vec{\boldsymbol{\Gamma}}_t(x_t)$ contains random variable sequences; relations and equalities in $\vec{\boldsymbol{\Gamma}}_t$ hold $\mathbb{P}$-almost everywhere (a.e.).

The standard approach to approximate the optimal policy function using $\mathbf{E}_t$ (i.e., Coleman-Reffett iteration, Coleman (1990); Reffett (1996); Li and Stachurski (2014)) can be seen as equivalent to numerically finding roots of $\mathbf{E}_t$ in terms of (y_t, μ_t) given m_t, over a regular exogenous grid of m_t values. Following Iyengar and Kang (2005) we refer to this as the *forward problem*. In contrast, the EGM has been informally understood to significantly speed up solution time by analytically inverting the FOCs of (**CS-BE**) to solve for m_t, over a regular exogenous grid of y_t values (Carroll, 2006). We extend the intuitive understanding of EGM to formally define an *inverse problem* as

$$\textbf{(IO-FOC)} \qquad \Theta_t^F(y_t, \mu_t) := \left\{ m_t \in M_t \,\middle|\, \mathbf{E}_t(y_t, \mu_t, m_t) = 0 \right\}, \qquad (y_t, \mu_t) \in Y_t \times \mathbb{R}_+^{N_g}.$$

Importantly, note we define the inverse problem Θ_t^F on a space that encompasses both post-states and multipliers that we collectively refer to as *observable variables*. This definition means the solutions to Θ_t^F are consistent with the optimal choice of binding constraints. However, $\Theta_t^F(y_t, \mu_t)$ may still contain multiple local optima: first, $\vec{\boldsymbol{d}}_t$ is not an argument for the maximization problem (**FS-DP**) and so, $\mathrm{v}_t^{\vec{\boldsymbol{d}}_t}$ is concave in the continuous state. Even if we fix d_t and d_{t+1}, though, v_{t+1} may feature 'secondary kinks' and not be concave in the continuous state as (i) the max operator over the non-convex set $\vec{\mathbf{\Gamma}}_{t+1}(x_{t+1})$ does not commute concavity, and (ii) v_{t+1} is the upper envelope over future discrete choices in $\vec{\mathbf{\Gamma}}_{t+1}(x_{t+1})$. Q_t will thus not be concave, leading to sub-optimal solutions in $\Theta_t^F(y_t, \mu_t)$.

The inverse problem consistent with global optima is then defined by

$$\textbf{(IO)} \qquad \Theta_t(y_t, \mu_t) := \left\{ m_t \in \Theta_t^F(y_t, \mu_t) \,\middle|\, \mathbf{d}_{t+1}(x_{t+1}) = \arg\max_{\vec{\boldsymbol{d}}'} \mathrm{Q}_t^{\vec{\boldsymbol{d}}'}(x_t, y_t, d_t) \right\},$$

where $(y_t, \mu_t) \in Y_t \times \mathbb{R}_+^{N_g}$, such that (1) holds, $\vec{\boldsymbol{d}}'$ is feasible, and the function $\mathbf{d}_{t+1}$ maps x_{t+1} to a sequence of discrete choices generated by the optimal policy functions. Before characterizing $\mathbf{E}_t$ and computing Θ_t, let us summarize the three critical challenges to using Euler equation methods currently.

2.2. **Euler equation challenges.**

Non-differentiability of the value function. Euler equations are typically characterized by differentiating the maximand in (**CS-BE**), which involves differentiating the agent's next period value function with respect to the continuous state. Note here that $\mathrm{v}_t(x_t) = \mathrm{u}_t(w_t, z_t, m_t, d_t, \mathrm{y}_t(m_t)) + \mathbb{E}_{x_t} \mathrm{v}_{t+1}(x_{t+1})$, where $x_{t+1} = \mathrm{F}_t(d_t, \mathrm{y}_t(m_t), w_{t+1})$ and y_t is the optimal policy function. If the agent's problem contains discrete choices and occasionally binding constraints, then (i) y_t may exhibit jump discontinuities (Dobrescu and Shanker, 2023) and kinks (Achdou et al., 2021), and (ii) $\partial_m \mathrm{v}_t$ may not be defined everywhere for every t (Iskhakov, 2015). Clausen and Strub (2020) attempts to overcome this issue by characterizing differentiability given an interior solution path away from the jump points. Interiority is, however, violated in many models. One such example is our second application in Section 6 where a subset of the occasionally binding constraints actually end up binding (see Rincón-Zapatero and

Santos (2009) and also Remark 6.1). Additionally, note that the method in Clausen and Strub (2020) also requires finding support functions, which may become very cumbersome in complex applications.

Differentiability of the value function is challenging, however, even in the absence of discrete choices. Prior attempts to characterize the Euler equation assumed compact feasibility correspondences and, at the same time, did not allow the reward function to reach $-\infty$ (Rincón-Zapatero and Santos, 2009; Rendahl, 2015; Marimon and Werner, 2021). We thus see existing results falling short of accommodating a wide range of realistic reward functions (Rincón-Zapatero, 2024). For instance, if feasibility correspondences are to be compact, then constant relative risk aversion (CRRA) utility functions (i.e., with CRRA parameter above 1) in income fluctuation models would require unbounded utility values that can reach $-\infty$ (Carroll, 2023).[7]

Invertibility of the Euler equation. While inverting the Euler equation can significantly improve efficiency, the challenge here lies in constructing the *exogenous grid* on which the Euler equation is invertible and Θ_t^F is non-empty. To this effect, we would need to characterize the subspace of $Y_t \times \mathbb{R}_+^{N_g}$ in which we can construct an arbitrarily dense grid as the exogenous grid. Up to our best knowledge, no formal result provides guidance on how to do so for problems with occasionally binding constraints or non-analytical inverses. Iskhakov (2015) gives conditions for when an analytical inverse of the Euler equation exists on the post-state space for problems without constraints. In a problem with constraints, Druedahl and Jørgensen (2017) points out that the policy functions must be an injection but does not provide specific conditions for the structure of the exogenous grid on which invertibility holds. To find the optimal binding constraints, the authors suggest evaluating the policy function via EGM for each possible combination of constraints. The optimal policy function is then determined by an *outer loop* that evaluates the value function on the state space for each possible such constraint combination. However, this outer loop leads to an unnecessary computational step that becomes costly in high-dimensional applications where the number of constraint combinations grows exponentially with each added constraint (such as in Dobrescu et al. (2024b) for instance). As we show in Section 4.2, the generalized Euler equation sharply characterizes the exogenous grid structure on which an inverse exists, and the optimal constraints that bind given the inverse solution. This avoids any extra upper envelope loops by inverting only from the image of the policy function optimized over the choice of constraints.

Non-concavity of the value function. Recall that even if one is able to correctly characterize the Euler equation and its inverse, $\Theta_t^F(y_t, \mu_t)$ may still contain multiple local optima. The presence of multiple local optima in Θ_t^F becomes a computational challenge because inverse methods do not evaluate all the possible roots of the Euler equation given fixed m_t. Methods proposed so far to approximate the upper envelope

[7] While Li and Stachurski (2014) and Ma et al. (2022) derive the Euler equation without such restrictions, they only (i) focus on specific applications, and (ii) assume bounded marginal utility and a strictly positive lower bound on earnings shocks. These approaches cannot, however, apply to models with a naturally arising liquidity constraint, such as the widely-used models featuring unemployment risk (Carroll, 2023).

of the local optima generated by inverting the Euler equation (Fella, 2014; Druedahl and Jørgensen, 2017; Iskhakov et al., 2017) have two key limitations. First, they cannot recover the upper envelope when exogenous and endogenous grids are irregular or the policy function is non-monotone. This limitation is significant since many widely used models (such as models of durable stock accumulation with fixed adjustment costs or models of consumer credit) have non-monotone policies and/or irregular exogenous grids (Section 6.2). Second, existing upper envelope methods do not provide any assurance of accuracy, asymptotic or otherwise, of the computed solution.[8]

3. Necessity and sufficiency of the generalized Euler equation

The generalized Euler equation. Let λ_t be current period shadow value of the continuous state, λ' the expected shadow value of next period state, and define S-function as

$$(\mathbf{S}) \quad \mathbf{S}_t(m_t, y_t, \mu_t, \lambda_t \mid \lambda') := \mathrm{u}_t(w_t, z_t, m_t, d_t, y_t) + \lambda' \cdot \mathrm{F}_t^m(d_t, y_t, w_{t+1}) - \lambda_t \cdot m_t + \mu_t \cdot \mathrm{g}_t(w_t, z_t, m_t, d_t, y_t), \qquad \lambda' \geq 0$$

where $m_t \in M_t, y_t \in Y_t, \mu_t \in \mathbb{R}_+^{N_g}$, and $\lambda_t \in \mathbb{R}_+^{N_M}$. At optimum, (i) the constraint multiplier μ_t is the vector of marginal values of relaxing the constraints, and (ii) the shadow value λ_t is the vector of the marginal values of increasing the start-of-period continuous states. Analogous to a deterministic discrete time version of the Hamiltonian (Sorger, 2015), the S-function represents a time-incremental value of the objective function as a function of the state and post-state. In a stochastic discrete time setting, however, arguments for the Hamiltonian become infinite-dimensional objects (Bewley, 1972; Dechert, 1982). In this case, the S-function can represent the multipliers, the shadow value, and the time-incremental value as functions of the real-valued current state *holding expectations over the future fixed in the term* λ'. This formulation avoids differentiating the value function, and avoids the need for abstract derivatives to derive the Euler equation. To proceed, given fixed variables ξ_t, we say $(m_t, y_t, \mu_t, \lambda_t)$ is a saddle point if (d_t, y_t) is feasible, and

$$(2) \quad \partial_m \mathbf{S}_t(m_t, y_t, \mu_t, \lambda_t \mid \lambda') = \partial_m \mathrm{u}_t(w_t, z_t, m_t, d_t, y_t) + \mu_t^\top \partial_m \mathrm{g}_t(w_t, m_t, z_t, d_t, y_t) - \lambda_t^\top = 0,$$

$$(3) \quad \partial_y \mathbf{S}_t(m_t, y_t, \mu_t, \lambda_t \mid \lambda') = \partial_y \mathrm{u}_t(w_t, z_t, m_t, d_t, y_t) + \mu_t^\top \partial_y \mathrm{g}_t(w_t, z_t, m_t, d_t, y_t) + \lambda'^{,\top} \partial_y \mathrm{F}_t^m(d_t, y_t, w_{t+1}) = 0,$$

$$(4) \quad \mu_t \circ \mathrm{g}_t(w_t, z_t, m_t, d_t, y_t) = 0, \qquad \mu_t \geq 0.$$

[8] Druedahl and Jørgensen (2017) offers a multidimensional algorithm that generates local triangulations on the endogenous grid by identifying triangles in the exogenous grid. The points retrieved by their method become asymptotically dense in the optimal grid, but there are no error bounds for approximations of the policy function. Additionally, the method cannot be applied when the exogenous grid is irregular, and it is also tied to local triangulation using simplices on the exogenous grid. Doing so precludes using off-the-shelf interpolation methods such as Gaussian process regressions (Lujan, 2023) and Delaunay triangulations (Chen and Xu, 2004).

Given the next period shadow value function $\lambda_{t+1}\colon X_t \to \mathbb{R}_+$ and given ξ_t, we use the FOC with respect to the post-state (3) and the complementary slackness condition (4) to define the generalized Euler equation. In particular, $\mathbf{E}_{y,t}(m,y,\mu)\colon = \partial_y \mathbf{S}(m,y,\mu,\lambda\,|\,\mathbb{E}_{w_t}\lambda_{t+1}(x'))$ and $\mathbf{E}_{\mu,t}(m,y,\mu)\colon = \mu \circ \mathrm{g}(w,z,m,d,y)$, where $x' = (w_{t+1}, z_{t+1}, m')$ and $m' = \mathrm{F}^m_t(d_t, y, w_{t+1})$.

Necessity and sufficiency. For the following assumptions, let $\{\mathrm{d}_t, \mathrm{y}_t\}_{t=0}^T$ be the solution to problem (**DP**).

Assumption 3.1. *$\forall\, x_t \in X_t$, there exists $\epsilon > 0$ s.t. $\mathrm{u}_t(w_t, z_t, \cdot, d_t, \cdot)$ is continuously differentiable on $\mathbb{B}_\epsilon((m_t, \mathrm{y}_t(x_t)))$, where $d_t = \mathrm{d}_t(x_t)$.*

Assumption 3.2. *$\forall\ (w_t, d_t) \in W_t \times D_t$, $\mathrm{F}^m_t(d_t, \cdot, w_{t+1})$ is affine.*

Assumption 3.3. *For $(m_t, y_t) \in K_{l,t}$, $\left|\left\{i \,\middle|\, \mathrm{g}_{i,t}(m_t, y_t) = 0\right\}\right| = \mathrm{rank}(\partial_y \mathrm{g}^l_t(m_t, y_t))$.*

Note that Assumptions 3.1 - 3.3 are unrestrictive (Rincón-Zapatero and Santos, 2009). However, as mentioned, our problem definition does not require real valued rewards ($\mathrm{u} > -\infty$) or compact-valued feasibility correspondences Γ_t, and we do not impose a bound on the marginal reward (i.e., utility) or shocks. Importantly, we also allow discrete choices.

We now confirm $\mathbf{E}_t\colon = \left[\mathbf{E}_{y,t}, \mathbf{E}_{\mu,t}\right]$ is a generalized Euler equation (see Definition 1). We start with a sufficient condition for a sequence of functions to be optimal policies. Consider a sequence of feasible functions $\{\mathrm{d}_t, \mathrm{y}_t\}_{t=0}^T$ and a sequence of non-negative multiplier and shadow value functions $\{\mu_t, \lambda_t\}_{t=0}^T$, with $\mu_t\colon X_t \to \mathbb{R}^{N_g}$ and $\lambda_t\colon X_t \to \mathbb{R}^{N_M}$. Let $\vec{\boldsymbol{d}}_0$ and $\{x_t, y_t\}_{t=0}^T$ be generated by $\{\mathrm{d}_t, \mathrm{y}_t\}_{t=0}^T$ and recall $x_t = (w_t, z_t, m_t)$.

Proposition 3.1. ***(Sufficient FOCs)***

(1) If, for all t and $x_t \in X_t$,
- *(i) $(m_t, \mathrm{y}_t(x_t), \mu_t(x_t), \lambda_t(x_t))$ is a saddle point of the S-function for $\lambda' = \lambda_{t+1}(x_{t+1})$,*
- *(ii) $\mathbb{E}_{x_0}\left[\lambda^2_{t+1}\right] < \infty$, $\mathbb{E}_{x_0}\left[\mu^2_t\right] < \infty$, $\mathbb{E}_{x_0}\left[m^2_t\right] < \infty$, and $\mathbb{E}_{x_0}\left[y^2_t\right] < \infty$, and*
- *(iii) $T < \infty$ or $\lim_{t\to\infty} \mathbb{E}_{x_0}\left[\lambda_{t+1}(x_{t+1})\right] = 0$,*

*then $\{\mathrm{y}_t\}_{t=0}^T$ solves (**FS-DP**) given $\vec{\boldsymbol{d}}_0$.*

*(2) In addition, if $\mathrm{d}_t(x_t), \vec{\boldsymbol{d}}_{t+1}, \mathrm{y}_t(x_t) = \arg\max_{d,\vec{\boldsymbol{d}}',y} \mathrm{Q}^{\vec{\boldsymbol{d}}'}_t(x_t, d, y)$ are s.t. $(d, \vec{\boldsymbol{d}}', y)$ is feasible, then $\{\mathrm{d}_t, \mathrm{y}_t\}_{t=0}^T$ solves (**DP**).*

Refer to online appendix E.1 for the proof.

With occasionally binding constraints (and without discrete choices), satisfying the Euler equation (i.e., Item (1). of Proposition 3.1) is sufficient. In the presence of discrete choices, Item (1). is sufficient given a sequence of future discrete choices. However, to solve (**DP**), the future stochastic sequence of discrete choices implied by the post-state choice must be optimal (i.e., Item (2). of Proposition 3.1 must also hold). In what follows, we show the main result of Section 3, which is that the generalized Euler equation is necessary.

Theorem 3.1. *(**Necessary FOCs**) If Assumption 2.1 and 3.1-3.3 hold, then there exist measurable functions* $\{\mu_t\}_{t=0}^T$ *and* $\{\lambda_t\}_{t=0}^T$*, with* $\mu_t \colon X_t \to \mathbb{R}_+^{N_g}$ *and* $\lambda_t \colon X_t \to \mathbb{R}_+^{N_M}$*, s.t.* $\forall t$*,* $(m_t,\ \mathrm{y}_t(x_t),\ \mu_t(x_t), \lambda_t(x_t))$ *is a saddle point of the S-function given* ξ_t *and* $\lambda' = \lambda_{t+1}(x_{t+1})$*.*
Refer to appendix A.3 for the proof.

Note that (2) defines the iteration of shadow value functions as

$$(\mathbf{L}) \qquad \lambda_t(x_t) = \nabla_m \mathrm{u}_t(w_t, z_t, m_t, \mathrm{d}_t(x_t), \mathrm{y}_t(x_t)) + \nabla_m \mathrm{g}_t(w_t, m_t, \mathrm{d}_t(x_t), \mathrm{y}_t(x_t))\mu_t(x_t).$$

While the value function may not be differentiable at the kink points (recall Section 2.2), the shadow value $\lambda_t(x_t)$ is a *supgradient* (i.e, $-\lambda_t(x_t)$ is a subgradient of $-\mathrm{v}_t^{\vec{d}_t}$, see online appendix D.2) to the value function conditional on a sequence of future discrete choices.

Corollary 3.1. *If Proposition 3.1 holds, then* $\mathrm{v}_t^{\vec{d}_t}(w_t, z_t, \tilde{m}_t) - \mathrm{v}_t^{\vec{d}_t}(w_t, z_t, m_t) \leq \lambda_t(x_t)(\tilde{m}_t - m_t)$ *for all* m_t*, with* $\tilde{m}_t \in M_t$*.*

Proof. Refer to online appendix E.2 for the proof. □

4. Invertibility of the generalized Euler equation

4.1. **Preliminaries.** In what follows, let ξ_t be fixed, $a_t = (y_{1,t}, \ldots, y_{N_Y,t}, \mu_{1,t} \ldots, \mu_{N_g,t})$ denote an end-of-period observed variable, and use $A_t = Y_t \times \Upsilon_t$ as the space of end-of-period observed variables, with $\Upsilon_t \subset \mathbb{R}_+^{N_g}$. Further, define a function $\sigma_t \colon X_t \to A_t$ mapping the state to observables, and whose evaluation satisfies $\sigma_t(x_t) = (\mathrm{y}_t(x_t), \mu_t(x_t))$, where μ_t is the multplier function. Moreover, we use $\sigma_t^{\vec{d}_{t+1}} = (\mathrm{y}_t^{\vec{d}_{t+1}}, \mu_t^{\vec{d}_{t+1}})$ to denote the function mapping the state to the observed variables given feasible current and future discrete choices $[d_t, \vec{d}_{t+1}]$.[9]

Finally, consider the following linear maps: for any two spaces X and Y, (i) let $\pi_Y \colon X \times Y \to Y$ denote a projection operator defined by the evaluation $\pi_Y(x, y) = y$, and (ii) fixing $x^\star \in X$, let $\mathrm{em}_Y \colon Y \to X \times Y$ denote the embedding $y \mapsto (x^\star, y) = \mathrm{em}_Y(y)$.

Active state spaces. The dimension of the continuous state space can often be reduced during computation.[10] To formalize the dimensionality reduction in our general setting, we consider the problem to have an *active state representation* if there exists (i) an *active state space* $\bar{M}_t \subset \mathbb{R}^{N_M}$ such that $\dim(\bar{M}_t) =: N_{\bar{M}} < N_M$, and (ii) a continuous selection function $\phi_t \colon M_t \to \bar{M}_t$ and policy function $\bar{\mathrm{y}}_t(\cdot|\xi_t) \colon \bar{M}_t \to Y_t$ such that if $\mathrm{y}_{d_t,t}$ is an optimal policy, then $\mathrm{y}_{d_t,t}(x_t) = \bar{\mathrm{y}}_t(\phi_t(m_t)|\xi_t)$ for all x_t and d_t. For any function f defined on the state space, we refer to its counterpart defined on the active state space as $\bar{\mathrm{f}}$. To streamline notation, we make the fixed variable argument of an

[9] Recall d_t is fixed so to streamline notation, we drop the subscript d_t from $\sigma_t^{\vec{d}_{t+1}}$, $\mathrm{y}_t^{\vec{d}_{t+1}}(x_t)$, and $\mu_t^{\vec{d}_{t+1}}(x_t)$.

[10] See for instance Fella (2014), where in a model with two wealth states (i.e., financial assets and housing), one overall wealth state becomes sufficient to compute the optimal policy for those who adjust housing stock.

active state space function implicit. For instance, we will write the evaluation of $\bar{\mathrm{f}}_t$ as $\bar{\mathrm{f}}_t(\bar{m}_t) \equiv \mathrm{f}_{d_t,t}(x_t)$, where $\bar{m}_t \equiv \phi_t(m_t)$.

Constrained regions. Let IB denote the set of all subsets of indices indexing the constraints on the active state space $\{\bar{\mathrm{g}}_{1,t} \ldots, \bar{\mathrm{g}}_{N_g,t}\}$. Fixing $\mathrm{IB}_l \in \mathrm{IB}$, let $\bar{\mathrm{g}}_t^l$ denote the vector of binding constraint functions. Solutions will then belong to different *constrained regions* $K_{l,t}$ associated with each subset $\mathrm{IB}_l \in \mathrm{IB}$ of binding constraints,

$$K_{l,t} := \left\{(\bar{m}_t, y_t) \in \mathrm{Gr}\bar{\Gamma}_t, \mu_t \in \Upsilon_t \,\middle|\, \bar{\mathrm{g}}_t^l(\bar{m}_t, y_t) = 0,\ \mu_t \circ \bar{\mathrm{g}}_t(\bar{m}_t, y_t) = 0\right\}. \tag{5}$$

The space $K_{l,t}^A := \pi_A K_{l,t}$ denotes the possible observables within a constrained region that we could invert from, and $K_t^A := \bigcup_{l \in \mathrm{IB}} \pi_A K_{l,t}$ is the space of observables satisfying the constraints and complementary slackness conditions (4).

4.2. **Main results on invertibility.** The main assumption required for invertibility is continuity of the policy function given a sequence of future discrete choices.[11]

Assumption 4.1. *For feasible $\vec{\boldsymbol{d}}_{t+1}$, the optimal policy function $\bar{\mathrm{y}}_t^{\vec{\boldsymbol{d}}_{t+1}}$ is continuous.*

Suppose we could construct an exogenous grid in an open neighborhood in Y_t and invert from it to a compact subset of the active state space (i.e., what we will call 'pure EGM'). We start with a necessary condition that tells us that for the inverse problem (**IO-FOC**) to be well-defined, the dimensions of the post-state space and active state space must be equal. For this result, let $\bar{\mathrm{y}}_t^{\vec{\boldsymbol{d}}_{t+1}}|_{\bar{C}}$ be the restriction of $\bar{\mathrm{y}}_t^{\vec{\boldsymbol{d}}_{t+1}}$ to the compact set $\bar{C} \subset \bar{M}_t$ with non-empty interior.

Claim 4.1. *Let 4.1 hold. If $\bar{\mathrm{y}}_t^{\vec{\boldsymbol{d}}_{t+1}}|_{\bar{C}}$ is injective, $\bar{\mathrm{y}}_t^{\vec{\boldsymbol{d}}_{t+1}}(\bar{C}) \subset \left\{y_t \,|\, \bar{\mathrm{g}}_t(\bar{m}, y_t) > 0, \bar{m} \in \bar{M}_t\right\}^{\mathrm{o}}$, and $\bar{\mathrm{y}}_t^{\vec{\boldsymbol{d}}_{t+1}}|_{\bar{C}}^{-1}$ is well-defined on a neighborhood in ${Y_t}^{\mathrm{o}}$, then $N_{\bar{M}} = N_Y$.*

Proof. By Assumption 4.1, $\bar{\mathrm{y}}_t^{\vec{\boldsymbol{d}}_{t+1}}|_{\bar{C}}$ is a homeomorphism, and so $\bar{\mathrm{y}}_t^{\vec{\boldsymbol{d}}_{t+1}}|_{\bar{C}}(\bar{C})$ and $\bar{C}$ are a homeomorphism with equal dimension. Setting $U \subset \bar{\mathrm{y}}_t^{\vec{\boldsymbol{d}}_{t+1}}|_{\bar{C}}(\bar{C})$ such that U is open in Y_t implies Y_t has the same dimension as $\bar{C}$ (see Proposition 3.5 in Lee (2011)). □

Claim 4.1 gives the minimum requirement on dimensionality for pure EGM to be well-defined, even in the absence of discrete choices. Since the restricted function $\bar{\mathrm{y}}_t^{\vec{\boldsymbol{d}}_{t+1}}|_{\bar{C}}$ can be injective even if $\bar{\mathrm{y}}_t^{\vec{\boldsymbol{d}}_{t+1}}$ is not, Claim 4.1 also applies to the general case where the policy function may not be globally invertible but is locally invertible.

Turning to the sufficient conditions for invertibility of pure EGM, by Claim 4.1, the space we invert from must be an $\mathbb{R}^{N_{\bar{M}}}$-dimensional submanifold of the observables. Fixing $\mathrm{IB}_l \in \mathrm{IB}$, we must then compute the inverse problem on a space of $N_{\bar{M}}$ *exogenous observables* such that $K_{l,t}$ has a non-empty interior along the dimensions of these

[11] Continuity here is benign since given a sequence of future discrete choices, (**FS-DP**) can be solved as a standard concave dynamic programming problem, yielding continuous policies. Feinberg et al. (2012) characterize existence and continuity even in the absence of bounded rewards or compact feasibility correspondences.

variables. We let (i) $\tilde{\mathrm{I}}_Y$ and $\tilde{\mathrm{I}}_\Upsilon$ denote the set of exogenous post-states and multipliers, respectively, and (ii) $\tilde{N}_Y$ and $\tilde{N}_g$ denote the indices of the exogenous post-states and multipliers, respectively.

Next, we define an embedding from the exogenous observables to the observable space. To do so, let $\tilde{Y}_t := \bigtimes_{i\in\tilde{\mathrm{I}}_Y} Y_{i,t}$, $\tilde{\Upsilon}_t := \bigtimes_{i\in\tilde{\mathrm{I}}_\mu} \Upsilon_{i,t}$, and $\tilde{A}_t = \tilde{Y}_t \times \tilde{\Upsilon}_t$. For a given a_t, note that we can fix the non-exogenous post-states taking on values in $Y_t \setminus \tilde{Y}_t$ along $N_Y - \tilde{N}_Y$ indices, and the non-exogenous multipliers taking on values in $\Upsilon_t \setminus \tilde{\Upsilon}_t$ along $N_g - \tilde{N}_g$ indices. We can then map the exogenous observables back to A_t using an embedding $\mathrm{em}_{\tilde{A}} \colon \tilde{A}_t \to A_t$.

Finally, we define a projection $\pi_{N_Y} \colon \mathbb{R}^{N_Y+N_g} \to \mathbb{R}^{N_Y}$ by selecting indices of the generalized Euler equation along which it is invertible. For this purpose, we select indices of derivatives in the vector $\bar{\mathbf{E}}_t = \left[\bar{\mathbf{E}}_{y,t}, \bar{\mathbf{E}}_{\mu,t}\right]$ as follows: (i) select indices of derivatives in $\bar{\mathbf{E}}_{y,t}$ with respect to the post-state such that $\partial_{y_i} \bar{\mathrm{g}}^l_t(\bar{m}_t, y_t) = 0$, and (ii) select indices of derivatives in $\bar{\mathbf{E}}_{\mu,t}$ associated with the binding constraints.[12] For what follows, fix $\mathrm{IB}_l \in \mathrm{IB}$ and assume λ_{t+1} is the next period shadow value function.

Theorem 4.1. ***(Invertibility of pure EGM)*** *If Assumptions 3.3 - 4.1 hold, $\tilde{N}_Y + \tilde{N}_g = N_Y = N_M$, and there exists*

(1) $\bar{m}_t \in {M_t}^{\mathrm{o}}$ and $(y_t, \mu_t) \in \left(K^A_{l,t}\right)^{\mathrm{o}}$ s.t. $y_t = \bar{\mathrm{y}}^{\vec{\boldsymbol{d}}_{t+1}}_t(\bar{m}_t)$ for feasible $\vec{\boldsymbol{d}}_{t+1}$, and

(2) given (y_t, μ_t), an embedding $\mathrm{em}_{\tilde{A}} \colon \tilde{A}_t \to A_t$ and projection $\pi_{N_Y} \colon \mathbb{R}^{N_Y+N_g} \to \mathbb{R}^{N_Y}$ s.t.

$$\det \partial_{\bar{m}} \pi_{N_Y} \bar{\mathbf{E}}_t\left(\bar{m}, \mathrm{em}_{\tilde{A}}(\tilde{a})\right) \neq 0, \qquad \forall (\bar{m}, \mathrm{em}_{\tilde{A}}(\tilde{a})) \in K_{l,t}, \tilde{a} \in \left(\pi_{\tilde{A}} K_{l,t}\right)^{\mathrm{o}}, \tag{6}$$

then for a continuous function φ and neighborhood $U \subset \tilde{A}_t \ni (\tilde{y}_t, \tilde{\mu}_t)$, if $\tilde{e} \in U \subset \left(\pi_{\tilde{A}} K_{l,t}\right)^{\mathrm{o}}$, then $\Theta^F_t(\varphi(\tilde{e}))$ is non-empty. Moreover, if $\bar{m} \in \Theta^F_t(\varphi(\tilde{e}))$, then $(\bar{m}, \varphi(\tilde{e})) \in K_{l,t}$.

Refer to appendix B for the proof.

If the interior of $K_{l,t}$ contains a solution $(\bar{m}_t, y_t, \mu_t)$, under Theorem 4.1, we can construct an arbitrarily dense exogenous grid in a neighborhood of $\pi_{\tilde{A}} K_{l,t}$. For $\tilde{a}$ in this grid, we are guaranteed to find $\bar{m}$ satisfying $\pi_{N_Y} \nabla \bar{\mathbf{S}}_t(\bar{m}, \mathrm{em}_{K^A}(\tilde{a}) \,|\, \lambda') = 0$, where $\lambda' = \mathbb{E}_{w_t} \lambda_{t+1}(x')$, $x' = (w_{t+1}, z_{t+1}, m')$, and $m' = \mathrm{F}^m_t(d_t, y, w_{t+1})$. To define the function φ in Theorem 4.1, for a permutation ϕ, the optimal policy given $\vec{\boldsymbol{d}}_{t+1}$ and $\bar{m}$ will then be $y = \left(y_{\phi_1}, \ldots, y_{\phi_{\tilde{N}_Y}}, y_{\phi_{\tilde{N}_Y+1},t}, \ldots, y_{\phi_{N_Y},t}\right)$, where $y = \pi_Y \mathrm{em}_{\tilde{A}} \tilde{a}$. Variables $y_{\phi_1}, \ldots, y_{\phi_{\tilde{N}_Y}}$ in the vector y are the exogenous post-states, while the remaining variables are the post-states we held fixed to their value in y_t. Under Assumption 3.3, we can then analytically recover the complete set of multipliers μ by finding the root of $\nabla_y \bar{\mathbf{S}}_t(\bar{m}, y, \cdot \,|\, \lambda')$ (see (31) in appendix). Importantly, the inverse solution will provide a state $\bar{m}$ such that the optimal solution given $\bar{m}$ and some $\boldsymbol{d}_{t+1}$ is in the region $K^A_{l,t}$.

[12] Under Assumption 3.3, the number of multipliers associated with the binding constraints is equal to the number of post-states such that $\partial_{y_i} \bar{\mathrm{g}}^l_t(\bar{m}_t, y_t) \neq 0$. As such, the sum of the number of post-states such that $\partial_{y_i} \bar{\mathrm{g}}^l_t(\bar{m}_t, y_t) = 0$ and of the number of multipliers associated with the binding constraints is equal to N_Y.

During computation, this avoids the need for any costly secondary upper envelope loops to choose the optimal constraint.

Remark 4.1. *Fix* $\text{IB}_l \in \text{IB}$ *and consider the setting of Theorem 4.1. Suppose* $\tilde{a}_t$ *is a point in the exogenous grid, and we find* $\bar{m}_t$ *such that* $\bar{m}_t \in \Theta_t^F(\varphi(\tilde{a}_t))$. *By Proposition 3.1, the observable* a_t, *with* $a_t = \varphi(\tilde{a}_t)$, *solves* (**FS-DP**) *given* $\bar{m}_t$.

So far, we described how to invert the generalized Euler equation and how to construct an exogenous grid around a solution point in $K_{l,t}$. To verify solution existence, we can apply the straightforward Poincaré-Miranda theorem (see online appendix Corollary F.1).

Finally, when the dimension of the active state space is strictly lower than the post-state space, pure EGM will not be well-defined. The question in this case is: if we were to invert back from an exogenous grid, what would the structure of the exogenous grid be?

Claim 4.2. *Let* $\bar{C} \subset M_t$ *be compact, and consider a* $\vec{\boldsymbol{d}}_{t+1}$. *If* $\sigma_t^{\vec{\boldsymbol{d}}_{t+1}}|_{\bar{C}}$ *is injective and continuous onto its own image, then for each feasible* $\vec{\boldsymbol{d}}_{t+1}$, $\dim(\sigma_t^{\vec{\boldsymbol{d}}_{t+1}}(\bar{C})) = N_{\bar{M}}$.

The proof is analogous to the proof for Claim 4.1 and omitted. Claim 4.2 tells us though that the exogenous grid dimension must be the same as the active state space dimension. Moreover, a $N_{\bar{A}}$-dimensional submanifold of A_t can be constructed as the graph of a smooth function from $N_{\bar{A}}$ exogenous observables to $\mathbb{R}^{N_g+N_Y-N_{\bar{A}}}$ defined by the level sets of $a \mapsto \pi_{N_Y}\bar{\mathbf{E}}_t(\bar{m}, a)$ (see online appendix Corollary F.2, and example in Section 6.2).

4.3. **Computation using the inverse problem.** We collect the elements needed for the policy function approximation via the inverse generalized Euler equation method in a tuple $(\Theta_t^F, (K_{l,t})_{l\in\text{IB}}, (\mathcal{A}_{l,t})_{l\in\text{IB}}, \kappa_t)$. The inverse problem Θ_t^F and the constrained regions $K_{l,t}$ are as above. The set of grid points $\mathcal{A}_{l,t}$ denotes the exogenous grid. Elements of $\mathcal{A}_{l,t}$ will be denoted by $a_{t,i}^{\#}$ and depending on the context, we use $a_{t,i}^{\#}$ and $(y_{t,i}^{\#}, \mu_{t,i}^{\#})$ interchangeably. We must have $\mathcal{A}_{l,t} \subset \bigcup_{\vec{\boldsymbol{d}}_{t+1}} \sigma_t^{\vec{\boldsymbol{d}}_{t+1}}(\bar{M}_t) \bigcap K_{l,t}$, where the union is taken over all future discrete choices such that $[d_t, \vec{\boldsymbol{d}}_{t+1}]$ is feasible given some $\bar{m}_t \in \bar{M}_t$. For each l, we can set up $\mathcal{A}_{l,t}$ to be a finite subset of an $N_{\bar{M}}$-dimensional space of exogenous observables in the image of the policy functions within the constrained region $K_{l,t}$. In practice, the points $\mathcal{A}_{l,t}$ can be set up as a space of variables (e.g., control variables) isomorphic to the observables (see Section 6.1).

The function κ_t is a continuous *grid pasting function* where $\kappa_t \colon \bigcup_{\vec{\boldsymbol{d}}_{t+1}} \sigma_t^{\vec{\boldsymbol{d}}_{t+1}}(\bar{M}_t) \to \mathbb{R}^{N_{\bar{M}}}$. This function allows us to join the different constrained regions into a single $N_{\bar{M}}$-dimensional space. Placing restrictions on the curvature of κ_t will be key in implementing the RFC algorithm and its asymptotic error bound. The choice of κ_t will be discussed below.

The computation of the inverse problem fixes an exogenous grid, aiming to obtain the corresponding endogenous grid $\mathcal{M}_t^\star \subset M_t$ by solving the inverse problem

(**IO**) such that $\bar{m}^{\#}_{t,i} \in \Theta_t(y^{\#}_{t,i}, \mu^{\#}_{t,i})\ \forall (y^{\#}_{t,i}, \mu^{\#}_{t,i}) \in \mathcal{A}_t, \bar{m}^{\#}_{t,i} \in \mathcal{M}_t$. Next, let $I^{\mathcal{A}}$ be the index set for the exogenous grid and $x^{\#}_{t,i} = (w_t, \bar{m}^{\#}_{t,i}, z_t)$. Additionally, let (i) the grid of objective values be denoted by $\mathcal{V}^{\star}_t = \left\{\mathrm{Q}_t(x^{\#}_{t,i}, d_{t,i}, y^{\#}_{t,i})\right\}_{i \in I^{\mathcal{A}}}$ that is obtained by evaluating (**Q**), and (ii) the optimal exogenous grid points be denoted by $\mathcal{A}^{\star}_t := \left\{y^{\#}_{t,i}, \mu^{\#}_{t,i} \in \mathcal{A}_t \middle| \Theta_t(y^{\#}_t, \mu^{\#}_{t,i}) \neq \varnothing\right\}$. The endogenous grid generated by the inverted Euler equation (**IO-FOC**) will be denoted by $\mathcal{M}^{\mathrm{F}}_t$, with $\mathcal{M}^{\mathrm{F}}_t \subset \bar{M}_t$, and satisfying $\bar{m}^{\#}_{t,i} \in \Theta^{\mathrm{F}}_t(y^{\#}_{t,i}, \mu^{\#}_{t,i}),\ \forall (y^{\#}_{t,i}, \mu^{\#}_{t,i}) \in \mathcal{A}_t, \bar{m}^{\#}_{t,i} \in \mathcal{M}^{\mathrm{F}}_t$. The objective values of the future choice-specific value functions can be collected in a grid $\mathcal{V}^{\mathrm{F}}_t = \left\{\mathrm{Q}_t(x^{\#}_{t,i}, d_t, y^{\#}_{t,i})\right\}_{i \in I^{\mathcal{A}}}$, obtained by evaluating (**Q**). Finally, let $\nabla\mathcal{V}^{\mathrm{F}}_t$ denote the supgradients of the future discrete choice-specific values $\mathcal{V}^{\mathrm{F}}_t$.

5. Rooftop-cut algorithm for discrete-continuous problems

Note that by Item (1). of Proposition 3.1, each exogenous grid point $a^{\#}_{t,i}$ implies a particular stochastic sequence of future discrete choices $\boldsymbol{d}_{t+1}$. We do not know, however, if this sequence is optimal given the current state implied by the endogenous grid point $\bar{m}^{\#}_{t,i}$ in $\mathcal{M}^{\mathrm{F}}_t$. The RFC algorithm uses the *supgradients of the future choice-specific value functions* in the $\nabla\mathcal{V}^{\mathrm{F}}_t$ grid to determine if neighboring points in the endogenous grid are optimal or not. To implement the algorithm, we set a jump detection threshold $\bar{J} > 0$, and a search radius $\rho_r > 0$. Let I^{F} be the index set of the points in $\mathcal{M}^{\mathrm{F}}_t$, and initialize $I^{\mathrm{cut}} \equiv \{\}$.

Box 1: RFC algorithm

For each $j \in I^{\mathrm{F}}$,

(1) Construct tangent $\bar{m}^{\#} \mapsto \nabla v^{\#}_{t,j} \circ (\bar{m}^{\#} - \bar{m}^{\#}_{t,j})$, with $\nabla v^{\#}_{t,j} \in \nabla\mathcal{V}^{\mathrm{F}}_t$.

(2) For each l such that $\bar{m}^{\#}_{t,l} \in \mathbb{B}_{\rho_r}(\bar{m}^{\#}_{t,j}) \cap \mathcal{M}^{\mathrm{F}}_t$, if

(i) the plane $\bar{m}^{\#} \mapsto \nabla v^{\#}_{t,j}(\bar{m}^{\#} - \bar{m}^{\#}_{t,j})$ dominates $v^{\#}_{t,l}$ at the endogenous grid point $\bar{m}^{\#}_{t,l}$ - i.e., $\nabla v^{\#}_{t,j} \circ (\bar{m}^{\#}_{t,l} - \bar{m}^{\#}_{t,j}) > v^{\#}_{t,l}$, and

(ii) the 'observable gradient' between j and l 'jumps' - i.e., $\frac{\kappa_t(a^{\#}_{t,j} - a^{\#}_{t,l})}{\|\bar{m}^{\#}_{t,l} - \bar{m}^{\#}_{t,j}\|} > \bar{J}$,

then append l to I^{cut}.

Constructing an index set $I^{\mathrm{RFC}} := I \setminus I^{\mathrm{cut}}$, the grids constructed by the RFC algorithm will then be $\mathcal{M}^{\mathrm{RFC}}_t := \left\{m^{\#}_{t,i}\right\}_{i \in I^{\mathrm{RFC}}}, \mathcal{A}^{\mathrm{RFC}}_t := \left\{a^{\#}_{t,i}\right\}_{i \in I^{\mathrm{RFC}}}$, and $\mathcal{V}^{\mathrm{RFC}}_t := \left\{v^{\#}_{t,i}\right\}_{i \in I^{\mathrm{RFC}}}$.

Figure 1 demonstrates the RFC algorithm for a stylized one-dimensional problem. Consider an unconstrained problem, and assume κ_t is the identity function.

Both panels show on the x-axis the endogenous grid points in $\mathcal{M}_t^{\mathrm{F}}$. On the y-axis, the left panel shows the points of the future choice-specific values in $\mathcal{V}_t^{\mathrm{F}}$, while the right panel shows the policy function values in the grid $\mathcal{Y}_t^{\mathrm{F}}$. Points $(\bar{m}^{\#}_{t,i-1}, v^{\#}_{t,i-1})$, $(\bar{m}^{\#}_{t,i}, v^{\#}_{t,i})$, $(\bar{m}^{\#}_{t,i+2}, v^{\#}_{t,i+2})$, and $(\bar{m}^{\#}_{t,i+3}, v^{\#}_{t,i+3})$ are on the upper envelope, while the points $(\bar{m}^{\#}_{t,i-1}, a^{\#}_{t,i-1})$, $(\bar{m}^{\#}_{t,i}, a^{\#}_{t,i})$, $(\bar{m}^{\#}_{t,i+2}, a^{\#}_{t,i+2})$, and $(\bar{m}^{\#}_{t,i+3}, a^{\#}_{t,i+3})$ define the optimal policy. In contrast, point $(\bar{m}^{\#}_{t,i+1}, v^{\#}_{t,i+1})$ is not on the upper envelope, and policy $(\bar{m}^{\#}_{t,i+1}, a^{\#}_{t,i+1})$ is not optimal. Here note that point $(\bar{m}^{\#}_{t,i+1}, a^{\#}_{t,i+1})$ 'jumps' from point $(\bar{m}^{\#}_{t,i}, a^{\#}_{t,i})$ (see the right panel) since it is associated with a different sequence of future discrete choices. Point $(\bar{m}^{\#}_{t,i+1}, a^{\#}_{t,i+1})$ is also dominated by the tangent to the future choice-specific value function at $(\bar{m}^{\#}_{t,i}, v^{\#}_{t,i})$ (see the left panel), and is thus removed. In contrast, while point $(\bar{m}^{\#}_{t,i+3}, a^{\#}_{t,i+3})$ also 'jumps' from the point $(\bar{m}^{\#}_{t,i}, a^{\#}_{t,i})$, this point dominates the tangent, and is thus retained. Point $(\bar{m}^{\#}_{t,i+4}, a^{\#}_{t,i+4})$ is similarly removed.

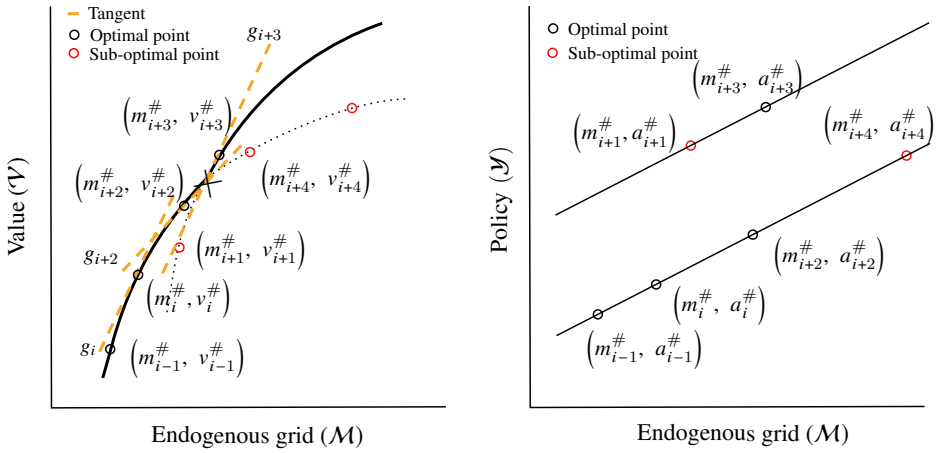

FIGURE 1. The RFC algorithm

How do we choose the pasting function κ_t, the jump detection threshold $\bar{J}$, and the search radius ρ_r? We briefly describe the practical considerations here and turn to a formal analysis in the next section. For each feasible sequence of future discrete choices $\boldsymbol{d}_{t+1}$, we require κ_t to be such that the function $\bar{\kappa}_t^{\boldsymbol{d}_{t+1}}$ defined by $\bar{m} \mapsto \kappa_t(\sigma_t^{\boldsymbol{d}_{t+1}}(\bar{m}))$ is Lipshitz with constant no greater than L_1, and has a Lipshitz inverse with constant no greater than L_2. This allows us to relate the exogenous grid spacing to the endogenous grid spacing. In many applications, the function mapping the exogenous observables to appropriately chosen controls (e.g., consumption) or post-states can serve as the evaluation of κ_t.[13]

[13]To fix intuition, take the case of an income fluctuation problem (Li and Stachurski, 2014) with no discrete choices, a liquid asset y_t, an artificial liquidity constraint $y_t \geq 0$, and i.i.d earnings shocks. We can set $\kappa_t(\mu, y) = \partial \mathrm{u}^{-1}(\mu + \mathbb{E}_{x_t}\lambda_{t+1}(\mathrm{F}_t^m(w_{t+1}, y)))$, where $\partial \mathrm{u}^{-1}$ is the inverse of the marginal utility and μ is the multiplier associated with the liquidity constraint.

The choice of the jump detection threshold can be made based on the maximum possible curvature of the functions $\bar{\kappa}_t^{\boldsymbol{d}_{t+1}}$ given a sequence of future discrete choices $\boldsymbol{d}_{t+1}$. For instance, in a standard income fluctuation problem, the marginal propensities to consume are bounded above by one and below by a constant that can be derived analytically (Carroll, 2023), allowing us to set $\bar{J} \geq 1$. The search radius, on the other hand, can be chosen to be greater than the maximum spacing between neighboring points in the endogenous grid. Consider constructing an exogenous grid such that for a particular grid size $|\mathcal{A}_t|$, there exists ϵ with $\|\bar{\kappa}_t^{\boldsymbol{d}_{t+1}}(a_{t,i}^{\#}) - \bar{\kappa}_t^{\boldsymbol{d}_{t+1}}(a_{t,j}^{\#})\| < \epsilon$ for neighboring exogenous points. Then the search radius can be set to $\rho_r = \epsilon L_2$ since the maximum possible distance between the associated endogenous grid points will be ϵL_2.

Finally, depending on the particular application, it may be more practicable to apply RFC iteratively or sequentially via search or scan methods to reduce the need to compute all pairwise tangent conditions. We discuss these practical implications in Section 6.

5.1. **Vectorization.** The deviation in the objective values between a point and its neighboring points can be written as $(\mathcal{V}_t - \mathcal{V}_t^{\text{neigh}})$, where $\mathcal{V}_t^{\text{neigh}}$ is a matrix such that each j^{th} row is a list of the objective values of the ι-neighboring points to j. Similarly, $|(\mathcal{Y}_t - \mathcal{Y}_t^{\text{neigh}})/(\mathcal{M}_t - \mathcal{M}_t^{\text{neigh}})|$ is the matrix of gradients of each policy value to neighboring policy values. The sub-optimal points can be computed via $I^{\text{cut}} = \left((\mathcal{M}_t - \mathcal{M}^{\text{neigh}_t}) \otimes \nabla\mathcal{V}_t > (\mathcal{V}_t - \mathcal{V}^{\text{neigh}_t})\right) \circ \left(|\mathcal{Y}_t - \mathcal{Y}^{\text{neigh}_t}|/\|(\mathcal{M}_t - \mathcal{M}^{\text{neigh}_t}\| > \bar{J}\right)$, where $\otimes$ is the appropriate tensor dot product.

5.2. **Convergence and error bound.** In what follows, Theorem 4.1 or Claim 4.2 will be in force. We further require the following assumptions: first, we require that the exogenous grid is a simplicial complex generated by the image of the grid pasting function.

Assumption 5.1. *For feasible* $\vec{\boldsymbol{d}}_{t+1}$, $\bar{\kappa}_t^{\vec{\boldsymbol{d}}_{t+1}}(\bar{M}_t \bigcap \mathcal{M}_t)$ *is a simplicial complex* $\mathbb{K}^{\vec{\boldsymbol{d}}_{t+1}}$.

Second, we require the exogenous grid to be asymptotically dense. Let $|\mathcal{A}_t|$ be the number of exogenous grid points, and let $\epsilon_{|\mathcal{A}_t|}$ denote the maximum circumcircle of simplicies in $\cup_{\vec{\boldsymbol{d}}_{t+1}} \mathbb{K}^{\vec{\boldsymbol{d}}_{t+1}}$.

Assumption 5.2. $\lim_{|\mathcal{A}_t| \to \infty} \epsilon_{|\mathcal{A}_t|} = 0$.

Third, we require that the policy functions translated by the pasting function (*conditional on a sequence of future discrete choices*) do not change arbitrarily fast. This assumption is rather standard in applications as quantities like marginal propensities to save and to consume are bounded (White, 2015; Carroll, 2023).

Assumption 5.3. *For all feasible $\boldsymbol{d}_{t+1}$ from M_t, the functions $\left\{\bar{\kappa}^{\boldsymbol{d}_{t+1}}\right\}_{\boldsymbol{d}_{t+1}}$ are bi-Lipshitz with Lipshitz constant of $\bar{\kappa}^{\boldsymbol{d}_{t+1}}$ no greater than L_1, and Lipshitz constant of $\bar{\kappa}^{\boldsymbol{d}_{t+1},-1}$ no greater than L_2.*

Next, let $C_0 = 1$ if each of the functions $\left\{\bar{\kappa}^{\boldsymbol{d}_{t+1}}\right\}_{\boldsymbol{d}_{t+1}}$ are monotone, and $C_0 = 2$ otherwise. Since (**FS-DP**) is concave, such monotonicity of $\bar{\kappa}^{\boldsymbol{d}_{t+1}}$ is standard (White, 2015) and sufficient (though not necessary) for an asymptotically dense simplicial complex in $\mathcal{M}_t^{\text{RFC}}$.

Assumption 5.4. *$C_0 L_2 \epsilon_{|\mathcal{A}_t|} \leq \rho_r$, and $\bar{J} = L_1$.*

For a measurable function f, define $\text{f} \circ \sigma_t^{\text{INT}}$ to be an approximation of $\text{f} \circ \sigma_t$ as follows: (i) for $\bar{m}_t \in \bar{M}_t$, if possible, linearly approximate $\text{f} \circ \sigma_t(\bar{m}_t)$ using Barycentric coordinates of a simplex from $\mathcal{M}_t^{\text{RFC}}$ enclosing $\bar{m}_t$, with circumradius of at least $L_2 \epsilon_{|\mathcal{A}_t|}$, (ii) otherwise approximate $\text{f} \circ \sigma_t(\bar{m}_t)$ using the nearest neighbor in $\mathcal{M}_t^{\text{RFC}}$. For the following result, let Assumptions 5.1 - 5.4 hold.[14]

Theorem 5.1. *(**Asymptotic error bound**) If W_j is finite for each j, then for $\bar{m}_t \in \bar{M}_t$ a.e., $\exists\ \bar{N}$ s.t. $\forall\, |\mathcal{A}_t| > \bar{N}$ we have: (i) if $D_t = 1\ \forall\, t$ then $\|\kappa_t \circ \sigma_t^{\text{INT}}(\bar{m}_t) - \kappa_t \circ \sigma_t(\bar{m}_t)\| < \epsilon_{|\mathcal{A}_t|}$, (ii) otherwise $\|\kappa_t \circ \sigma_t^{\text{INT}}(\bar{m}_t) - \kappa_t \circ \sigma_t(\bar{m}_t)\| < C_0 \epsilon_{|\mathcal{A}_t|}(L_2 L_1 + 1)$.*

Refer to appendix C for the proof.

Note that the assumption of a finite shock space is straightforward to satisfy in applications if, for instance, a discrete shock grid is used. Moreover, while this is a worse-case pointwise result, it implies that if the functions $\kappa_t \circ \sigma_t$ are bounded, then the moment conditions will converge as the exogenous grid size increases.

Corollary 5.1. *If $\left[\kappa_t \circ \sigma_t^{\vec{\boldsymbol{d}}_{t+1}}(\bar{m}_t)\right]^p$ is uniformly bounded for all feasible $\vec{\boldsymbol{d}}_{t+1}$, then for $p \geq 1$, $\mathbb{E}\left[\kappa_t \circ \sigma_t^{\text{INT}}(\bar{m}_t)\right]^p \to \mathbb{E}\left[\kappa_t \circ \sigma_t(\bar{m}_t)\right]^p$ as $|\mathcal{A}_t| \to \infty$.*

6. Applications

6.1. **Application 1: Savings and retirement choice.** Our first application is the model in Druedahl and Jørgensen (2017) to which we add an extra constraint to (i) demonstrate the RFC performance, and also (ii) show how using Theorem 4.1 to determine where constraints bind *on the exogenous grid* can significantly improve computational speed and deal with the added complexity.

Model environment. Let T be finite. Consider an agent who chooses a post-state $y_t = (y_{f,t}, y_{p,t})$ that consists of end-of-period financial assets $y_{f,t}$ and pension assets $y_{p,t}$ to maximize lifetime utility. The continuous state variables are start-of-period financial assets $m_{f,t}$ and pension assets $m_{p,t}$; the continuous state space is $M_t = M_{f,t} \times M_{p,t} = \mathbb{R}_+^2$ and the post-state space is $Y_t = Y_{f,t} \times Y_{p,t} = \mathbb{R}_+^2$. Each period,

[14] Including intersection points (Iskhakov et al., 2017; Dobrescu and Shanker, 2023) is at best subject to the error bound above as they rely on constructing secants between overlapping future choice-specific value functions.

the agent chooses whether to work next period, with $d_t = 1$ denoting employment and $d_t = 0$ retirement. The discrete state variable z_t captures the agent's start-of-period employment status. Accordingly, the discrete choice space and state space are $D_t = \{0, 1\}$ and $Z_t = \{0, 1\}$, respectively.

Turning to the transition functions, we note that financial assets evolve according to

$$m_{f,t+1} = (1 + r_f)y_{f,t} + z_{t+1}w_{t+1} + (1 - z_{t+1})\left(\bar{w} + (1 + r_p)y_{p,t}\right), \tag{7}$$

where $\bar{w}$ is the unemployment benefit paid to retirees. The rate of return on financial assets is r_f, and the rate of return on pension assets is r_p. If an agent is employed at the beginning of a period, they receive stochastic earnings w_t, with w_t being log-normally distributed. If, however, the agent retires, they receive their pension balance as a lump-sum payment. The transition function for pension assets is then given by

$$m_{p,t+1} = z_{t+1}(1 + r_p)y_{p,t}, \tag{8}$$

where pension assets only accumulate for workers. Each period the agent works ($z_t = 1$), they can make pension contributions $c_{p,t}$ that translate to end-of-period pension assets as

$$y_{p,t} = m_{p,t} + \chi(c_{p,t}), \tag{9}$$

where χ is a function representing the incentives to make pension contributions, with $\chi(x) = 1 + \bar{\chi}\log(1 + x)$, $\bar{\chi} > 0$. Finally, employment status evolves according to $z_{t+1} = d_t z_t$ and so, a retired agent cannot work again.

The feasibility correspondence for Γ_t is given by (i) the borrowing constraint on total assets $y_t \geq 0$, (ii) the liquidity constraint preventing pre-retirement pension withdrawals

$$\chi^{-1}(y_{p,t} - m_{p,t}) \geq 0, \tag{10}$$

(iii) the constraint preventing retirees from making further pension contributions

$$y_{p,t}(1 - z_t) = 0, \tag{11}$$

and (iv) a constraint that caps pension contributions to be no greater than earnings

$$c_{p,t} \leq w_t. \tag{12}$$

In what follows we will use constraint (iv) to demonstrate the utility of Theorem 4.1. While new compared to Druedahl and Jørgensen (2017), this constraint captures a key feature of many pension plans such as the 401(k) in the U.S. and superannuation plans in Australia.

Turning to payoffs, the agent enjoys consumption according to a CRRA utility function ν with parameter $\rho > 1$, and discounts time according to a factor $\beta \in (0, 1)$. An agent who remains employed pays a utility cost $\delta > 0$. For a worker who continues working, the Bellman equation is $\mathrm{v}_{1,t}(w_t, 1, m_{f,t}, m_{p,t}) = \max_{y_t \in \Gamma_t(x_t)} \left[\frac{c_t^{\rho-1}}{\rho-1} + \beta \mathbb{E}_{x_t} \mathrm{v}_{t+1}(w_{t+1}, 1, m_{f,t+1}, m_{p,t+1})\right] - \delta$, where $c_t = m_{f,t} - y_{f,t} - c_{p,t}$. For a worker who retires, $\mathrm{v}_{0,t}(w_t, 1, m_{f,t}, m_{p,t}) = \max_{y_t \in \Gamma_t(x_t)} \left[\frac{c_t^{\rho-1}}{\rho-1} + \beta \mathbb{E}_{x_t} \mathrm{v}_{t+1}(0, m_{f,t+1})\right]$. The

current discrete choice is $d_t = \arg\max_{d\in\{0,1\}} \mathrm{v}_{d,t}(w_t, 1, m_{f,t}, m_{p,t})$. The decision problem for the retiree is standard and we omit it for brevity (Druedahl and Jørgensen, 2017).

Euler equation and exogenous grid. The function ν is unbounded below since agents can consume an arbitrarily small amount. If $m_{f,t} > 0$, then for $\Gamma_t(x_t)$ to be compact-valued, $\Gamma_t(x_t)$ must include the feasible choice of zero consumption where utility hits $-\infty$. Conversely, if we exclude zero consumption from the feasible choices given x_t, then $\Gamma_t(x_t)$ will not be compact-valued. So even without non-differentiability due to discrete choices, Rincón-Zapatero and Santos (2009) cannot be applied to derive the Euler equation. Additionally, Clausen and Strub (2020) cannot be applied either since the solution will not always be an interior point in $\Gamma_t(x_t) \cap \Gamma_{t+1}^{-1}(y_{t+1})$, because (10) may bind in consecutive periods. We can, however, use the S-function to derive the Euler equation. To do so, note Assumptions 3.1 - 3.3 hold, let $\mathrm{u}_t(w_t, z_t, m_t, d_t, y_t) = \beta^t \frac{c_t^{\rho-1}}{\rho-1} =: \beta^t \nu(c_t)$, write the shadow values and multipliers in current value form, and consider

$$\nu'(c_t) = \mu_{f,t} + \beta \mathbb{E}_{x_t} \mathrm{u}'_{t+1}(c_{t+1}) \left(1 + r_f\right) = \mu_{f,t} + \beta \mathbb{E}_{x_t} \lambda_{t+1,f} \left(1 + r_f\right) \tag{13}$$

$$\nu'(c_t) = \mu_{p,t} - \mu_{\bar{p},t} + \mathbb{E}_{x_t} \lambda_{p,t+1} \left(1 + r_p\right) \left(1 + \chi'(c_{p,t})\right) \tag{14}$$

$$\mu_{f,t} y_{f,t} = 0 \tag{15}$$

$$\mu_{p,t} c_{p,t} = 0 \tag{16}$$

$$\mu_{\bar{p},t} \left(c_{p,t} - w_t\right) = 0 \tag{17}$$

$$\lambda_{p,t} = z_t \mathbb{E}_{x_t} \lambda_{p,t+1} \left(1 + r_p\right) + (1 - z_t) \nu'(c_t) \tag{18}$$

$$\lambda_{f,t} = \nu'(c_t) \tag{19}$$

where $c_t = m_{f,t} - y_{f,t} - c_{p,t}$, and $c_{p,t} = y_{p,t} - m_{p,t} - \chi(c_{p,t})$. The multiplier $\mu_{f,t}$ is associated with the borrowing constraint on financial assets ($y_{f,t} \geq 0$), the multiplier $\mu_{p,t}$ is associated with the pension withdrawal constraint (10), and $\mu_{\bar{p},t}$ is associated with the pension contributions cap constraint (12). For a worker, there are six combinations of binding constraints defined by $y_t \geq 0$, (10) and (12). We index the binding constraints by $\mathrm{IB} = \left\{\mathrm{ucon}, \mathrm{dcon}, \mathrm{acon}, \mathrm{con}, \overline{\mathrm{dcon}}, \overline{\mathrm{con}}\right\}$. By Theorem 4.1, we can construct each region, its corresponding exogenous observables, associated grids, and projection π_{N_Y} as [15]

- ucon: No constraints bind. $K^A_{\mathrm{ucon},t} = \left\{a_t \,|\, y_{f,t} \geq 0, y_{p,t} \geq 0, \mu_t = 0\right\}$, $\mathcal{A}_{\mathrm{ucon},t} \subset \{y_t \,|\, y_t \geq 0\}$. Exogenous observables are $y_{f,t}$, $y_{p,t}$; $\pi_{N_Y} \mathbf{E}_t$ is given by (13), (14).
- dcon: Lower pension constraint (10) binds. $K^A_{\mathrm{dcon},t} = \left\{a_t \,|\, y_t \geq 0, \mu_{f,t} = 0, \mu_{p,t} \geq 0, \mu_{\bar{p},t} = 0\right\}$, $\mathcal{A}_{\mathrm{dcon},t} \subset \{y_t | y_t \geq 0\}$. Exogenous observables are $y_{f,t}$,$y_{p,t}$; $\pi_{N_Y} \mathbf{E}_t$ is given by (13), (16).
- acon: Borrowing constraint binds ($y_{f,t} \geq 0$). $K^A_{\mathrm{acon},t} = \left\{a_t \,|\, y_{f,t} = 0, y_{p,t} \geq 0, \mu_{f,t} \geq 0, \mu_{p,t}, \mu_{\bar{p},t} = 0\right\}$, $\mathcal{A}_{\mathrm{acon},t} \subset$

[15] Recall that exogenous grids $\mathcal{A}_{l,t}$ are constructed as points equivalent to the exogenous observables. Formally, for instance, $\mathcal{A}_{\mathrm{acon},t} \subset \left\{y_{p,t}, c_t \,|\, y_{p,t} \geq 0, c_t \geq 0\right\} \cong \left\{y_{p,t}, \mu_{f,t} \,|\, y_{p,t} \geq 0, \mu_{f,t} \geq 0\right\}$.

$\{y_{p,t}, c_t \mid y_{p,t} \geq 0, c_t \geq 0\}$. Exogenous observables are $\mu_{f,t}$, $y_{p,t}$; $\pi_{N_Y}\mathbf{E}_t$ is given by (14), (15).

- con: All lower constraints bind. $K^A_{\text{con},t} = \{a_t | y_{f,t} = 0, y_{p,t} \geq 0, \mu_{f,t} \geq 0, \mu_{p,t} \geq 0, \mu_{\bar{p},t} = 0\}$, $\mathcal{A}_{\text{con},t} \subset \{y_{p,t}, c_t \mid y_{p,t} \geq 0, c_t \geq 0\}$. Exogenous observables are $y_{p,t}$, $\mu_{f,t}$; $\pi_{N_Y}\mathbf{E}_t$ is given by (15), (16).
- $\overline{\text{dcon}}$: Pension cap constraint (12) binds. $K^A_{\overline{\text{dcon}},t} = \{a_t \mid y_t \geq 0, \mu_{f,t} = 0, \mu_{p,t} = 0, \mu_{\bar{p},t} \geq 0\}$, $\mathcal{A}_{\overline{\text{dcon}},t} \subset \{y_t \mid y_t \geq 0\}$. Exogenous observables are $y_{f,t}$, $y_{p,t}$; $\pi_{N_Y}\mathbf{E}_t$ is given by (13), (17).
- $\overline{\text{con}}$: Borrowing and pension cap constraints ($y_{f,t} \geq 0$ and 12) bind. $K^A_{\overline{\text{con}},t} = \{a_t \mid y_{f,t} = 0, y_{p,t} \geq 0, \mu_{f,t} \geq 0, \mu_{p,t} = 0, \mu_{\bar{p},t} \geq 0\}$, $\mathcal{A}_{\overline{\text{con}},t} \subset \{y_{p,t}, c_t \mid y_t \geq 0\}$. Exogenous observables are $y_{p,t}$, $\mu_{f,t}$; $\pi_{N_Y}\mathbf{E}_t$ is given by (13), (17).

The first four constrained regions are common with Druedahl and Jørgensen (2017), while $\overline{\text{dcon}}$ and $\overline{\text{con}}$ arise due to the pension cap constraint. Additionally, note that to formally define the regions as above, we required the multipliers to obey the complementary slackness conditions (4). In general, additional constraints can lead to an exponential increase in the number of regions. The core idea of Theorem 4.1 is that by evaluating the inverse operator $\mathbf{\Theta}^F_t$ at exogenous grid points in each region, we are able to obtain prior information on the optimal constraint choice that binds from the exogenous grid. This means we do not need to interpolate separate policy functions for each constrained region across all possible exogenous grid points. A number of grid points are thus eliminated since they are not solutions to $\mathbf{\Theta}^F_t$, and the remaining points across the regions can be combined into a single irregular exogenous grid over which we need to apply an upper envelope method, and interpolate only once regardless of the number of constraints. (In the online appendix we verify that by Theorem 4.1 and Proposition F.1, we can construct an exogenous grid $\mathcal{A}_t$ around a solution point in the two-dimensional regions above.)

Finally, we can choose end-of-period pension assets and consumption evaluated at the exogenous grid, denoted by $a \mapsto (\hat{y}_{p,t}(a), \hat{c}_t(a))$, as the grid pasting function κ_t. The functions $\vec{\kappa}^{\vec{d}_{t+1}}_t$ are then the pension policy function and the consumption function $(y^{\vec{d}_{t+1}}_{p,t}, c^{\vec{d}_{t+1}}_t)$. Since the marginal propensity to consume (MPC) of $c^{\vec{d}_{t+1}}_t$ will be bounded above by 1 and the slope of $y^{\vec{d}_{t+1}}_{p,t}$ bounded above by 2, we can set $\bar{J} > 2$. Letting M_t be compact, the inverse of $(y^{\vec{d}_{t+1}}_{p,t}, c^{\vec{d}_{t+1}}_t)$ will also be Lipshitz and L_2 will be bounded above by $\frac{1}{\underline{\text{MPC}}}$, where $\underline{\text{MPC}}$ is the lower bound on the MPC (Carroll, 2023). We can thus pick $\rho_r > \frac{2\epsilon}{\underline{\text{MPC}}}$ as the search radius, where ϵ is the distance between exogenous grid points in '(y_t, c_t)-space'.

Numerical implementation. To illustrate the RFC algorithm, we use the baseline calibration in Druedahl and Jørgensen (2017), both with and without a pension cap. To benchmark our method, we implement the solution algorithm using (i) the nested EGM suggested by Druedahl (2021) (NEGM), (ii) EGM using our RFC algorithm

and a Delaunay triangulation (RFC w. Delaunay), and (iii) EGM using the upper envelope method in Druedahl and Jørgensen (2017) (G2EGM). To implement RFC efficiently, we apply the vectorized algorithm iteratively to nearest neighbors of a subset of total points in the endogenous grid until no new sub-optimal points are found.

Figure 2 shows the constrained segments in a model without a pension cap, from the set IB within both the endogenous and exogenous grid at time $t = T - 13$. Each region of the exogenous grid in the right panel is a two-dimensional submanifold of the space of observable variables, defined by the sets $K_{l,t}$. The sub-optimal red points are points within the regions that are removed by the RFC algorithm. Our contribution in Theorem 4.1 showed that inverting from these regions leads to the optimal solution. Note that while different constrained regions overlap in the exogenous grid, they form disjoint segments in the endogenous grid (i.e., each point in the endogenous grid is associated with a unique optimal solution and a unique optimal constraint choice). With two additional constrained regions, since the regions are disjoint in the endogenous grid, the number of endogenous grid points that the RFC with the interpolation step must process does not increase.

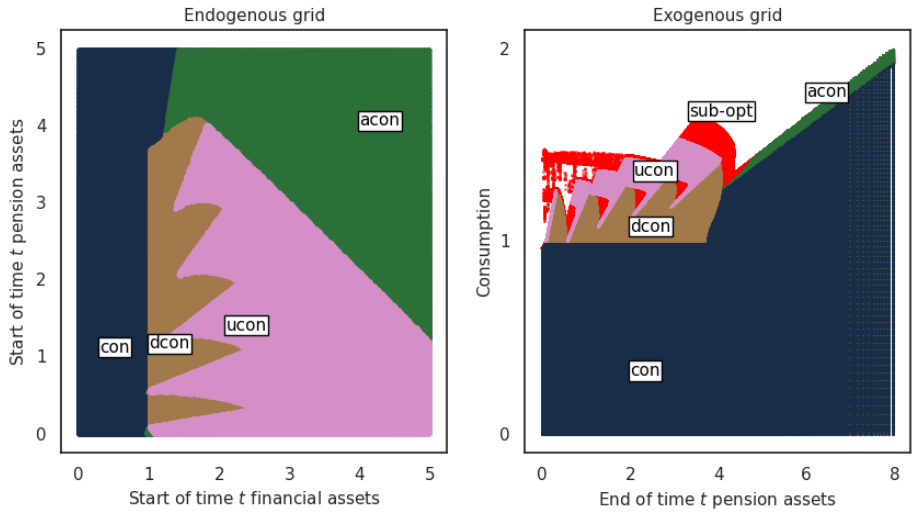

FIGURE 2. Constrained regions with no cap on pensions

In terms of accuracy, we find that our RFC implementation is comparable to the upper envelope method in terms of relative Euler error (see Figure H.1), and even dominates slightly on the mean Euler error (see online appendix). Turning to speed, the left panel of Figure 3 shows the time it takes to solve the model without a pension cap for 15 periods. We see that our implementation (i.e., RFC with interpolation via Delaunay triangulation) and the upper envelope method (G2EGM) are comparable in terms of total time efficiency, and both are about twice as fast as NEGM. Note here, however, also that the time actually taken by the RFC alone is about 25% of the total time. This gain in speed, due to the vectorized RFC and calculating the optimal constraints from the exogenous grid, also allows us to use an off-the-shelf

SciPy implementation of Delaunay triangulation to interpolate over the endogenous grid, significantly simplifying the implementation of the inverse method. [16]

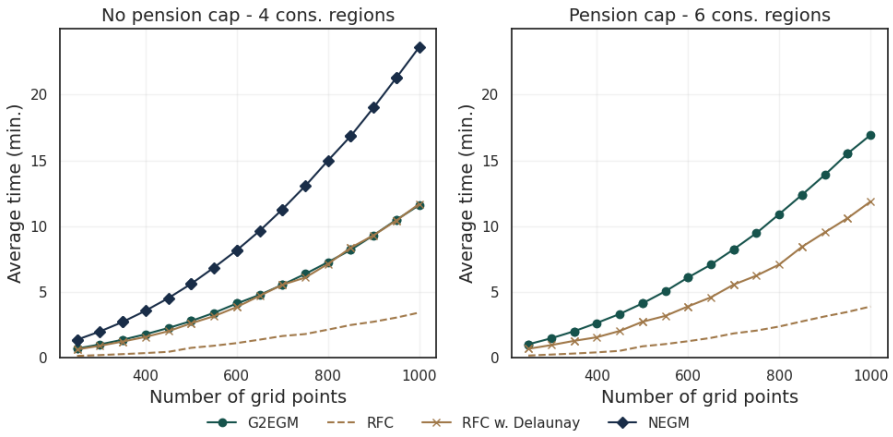

FIGURE 3. Computational speed benchmarking

Finally, the right panel of Figure 3 shows how our implementation handles two additional constrained regions. The time taken to invert the Euler equation and run RFC in this case remains almost identical to the one without the additional regions, since we already have the optimal points that are not constrained from the exogenous grid. So we only need to perform the upper envelope step using RFC and interpolate once over a similar number of grid points as when we had only four constrained regions. If we did not use Theorem 4.1, however, and evaluated the upper envelope of each region's policy function separately as in Druedahl and Jørgensen (2017), we would have a 50% increase in total computational time due to the 50% increase in the number of constrained regions.

6.2. **Application 2: Housing investments with adjustment frictions.** We now demonstrate our results in the context of a veritable workhorse model in the housing frictions literature (Kaplan and Violante, 2014; Yogo, 2016; Dobrescu et al., 2024b). To maintain comparability, we closely follow Druedahl (2021). While this model also features two dimensions of savings - one for liquid (financial) assets and one for illiquid (housing) assets - pure EGM cannot be applied. Rather, optimal financial and housing assets occupy one-dimensional submanifolds of the post-state space. In this case, we show EGM can still be employed to gain significant speed and numerical accuracy, using a root-finding step to construct an exogenous grid.

Model environment. Let T be finite. Consider an agent who chooses a post-state $y_t = (y_{f,t}, y_{h,t})$ consisting of end-of-period financial assets $y_{f,t}$ and housing assets $y_{h,t}$. The continuous state variables are start-of-period financial assets $m_{f,t}$ and housing

[16] Delaunay triangulations are the optimal triangulation on an irregular grid (Chen and Xu, 2004). While Druedahl and Jørgensen (2017) and Ludwig and Schön (2018) note that Delaunay may be computationally costly, this example shows how appropriate software libraries can make Delaunay triangulations highly efficient.

assets $m_{h,t}$; the post-state space is $Y_t = Y_{f,t} \times Y_{h,t} = \mathbb{R}^2_+$, and the continuous state space is $M_t = M_{f,t} \times M_{h,t} = \mathbb{R}^2_+$. The agent also makes a discrete choice d_t, where investing in and out of housing stock can only be made if $d_t = 1$. If $d_t = 0$ then $y_{h,t+1} = m_{h,t+1}$, and we must have

$$(y_{h,t} - m_{h,t})(1 - d_t) = 0. \tag{20}$$

Investments can be made in and out of the stock of $m_{f,t}$ without friction. Turning to the transition functions, financial assets evolve according to

$$m_{f,t+1} = (1 + r)y_{f,t} + w_{t+1}, \tag{21}$$

where financial assets earn a rate of return r, and w_{t+1} denotes stochastic earnings. We assume that housing brings no returns so

$$m_{h,t+1} = y_{h,t+1}, \tag{22}$$

and that the equations describing the non-negativity constraint on total resources $y_t \geq 0$ and the friction on housing $(y_{h,t} - m_{h,t})(1 - d_t) = 0$ define the value of the feasibility correspondence $\Gamma_t(x_t)$. Turning to per-period rewards, the agent enjoys utility from non-housing consumption c_t and end-of-period housing stock $y_{h,t}$. We assume per-period rewards are[17]

$$\mathrm{u}_t(m_t, y_t) = \beta^t \underbrace{\left[\frac{c_t^{\rho-1} - 1}{\rho - 1} + (1 - \alpha) \ln(y_{h,t}) \right]}_{\text{}},$$

$$s.t. \qquad c_t = m_{f,t} + d_t m_{h,t} - y_{a,t+1} - d_t(1 + \tau)y_{h,t+1}. \tag{23}$$

Adjusting the housing stock to $y_{h,t}$ requires paying $\tau y_{h,t}$ (with $\tau > 0$), leading to a non-concave continuation value. Thus, Bellman equation for an agent deciding not to adjust housing stock is $\mathrm{v}_{0,t}(w_t, m_t) = \max_{y_t \in \Gamma_t(x_t)} \left\{ \mathrm{v}_t(c_t, y_{h,t}) + \beta \mathbb{E}_{x_t} \mathrm{v}_{t+1}(w_{t+1}, m_{a,t+1}, m_{h,t}) \right\}$, where $c_t = m_{f,t} - y_{f,t}$. For an agent adjusting their housing stock, $\mathrm{v}_{1,t}(w_t, m_{f,t}, m_{h,t}) = \max_{y_t \in \Gamma_t(x_t)} \left\{ \mathrm{v}_t(c_t, y_{h,t}) + \beta \mathbb{E}_{x_t} \mathrm{v}_{t+1}(w_{t+1}, m_{a,t+1}, m_{h,t+1}) \right\}$, where $c_t = m_{f,t} + m_{h,t} - y_{f,t} - (1 + \tau)y_{h,t+1}$. For both Bellman equations, (21) - (23) must hold. The discrete choice is $d_t = \arg \max_{d \in \{0,1\}} \mathrm{v}_{d,t}(w_t, m_{f,t}, m_{h,t})$.

Euler equation and exogenous grid. The following remark shows that Theorem 6 by Clausen and Strub (2020) cannot be applied to derive the Euler equation since the next period policy in the one-shot deviation problem may not be in the feasible set's interior.

Remark 6.1. *If $d_{t+1} = 0$, then $(d_{t+1}, y_{t+1}) \in \Gamma_{t+1}(x_{t+1})$ if and only if $y_{h,t+1} = m_{h,t+1}$, and so $y_{h,t}$ cannot belong to the interior of $\left\{ y \mid d_{t+1}, y_{t+1} \in \Gamma_{t+1}(\mathrm{F}_t^m(d_t, y, w_{t+1})) \right\}$.*

However, Assumptions 3.1 - 3.3 hold. Using the S-function, for $t < T$, the Euler equation for financial assets is

$$\partial_c \mathrm{v}(c_t, y_{h,t}) = \mu_{a,t} + \beta \mathbb{E}_{x_t} \lambda_{a,t+1}(w_{t+1}, m_{f,t+1}, m_{h,t+1}) \geq \beta(1 + r) \mathbb{E}_{x_t} \partial_c \mathrm{v}(c_{t+1}, y_{h,t+1}), \tag{24}$$

[17] To ease exposition, in what follows we assume separable utility from housing and non-housing consumption. A CES specification is computationally simple to implement; our online repository provides an example.

where c_t and c_{t+1} obeys (23), and the state transition equations (21) - (22) hold. Note also that in the last term in (24), the optimal $t+1$ policy function is $y_{t+1} = \mathrm{y}_{t+1}(w_{t+1}, m_{f,t+1}, m_{h,t+1})$. If $d_t = 1$, the recursive Euler equation for housing stock is

$$(1+\tau)\partial_c \mathrm{v}(c_t, y_{h,t}) = \mu_{h,t} + \beta \mathbb{E}_{x_t} \lambda_{h,t+1}(w_{t+1}, m_{f,t+1}, m_{h,t+1}) + \partial_{y_h} \mathrm{v}(c_t, y_{h,t}) \geq \mathbb{E}_{x_t}\left[\sum_{k=t}^{\iota-1} \beta^{t-k} \partial_{y_h} \mathrm{v}(c_k, y_{h,k})\right] + \mathbb{E}_{x_t} \beta^{t-\iota} \partial_c \mathrm{v}(c_\iota, y_{h,\iota}). \tag{25}$$

The intuition of the financial assets Euler equation (24) is standard. The housing Euler equation (25), however, features a stochastic time subscript ι defined as the next period $d_\iota = 1$, meaning the housing stock shadow value is the discounted expected value of the stock *when this is next liquidated*, along with the stream of housing services provided up to the time of liquidation. (Section 4.1 in Kaplan and Violante (2014) gives a similar intuition.)

Suppose we know v_{t+1} and $\lambda_{h,t+1}$. We can first apply standard EGM with RFC to evaluate $y_{f,0,t}$ for *non-adjusters*, since only one Euler equation - i.e., (24) - will hold. For each possible time t housing state $m_{h,t}$ in the housing grid $\mathcal{Y}_{h,t}$ and exogenous state w_t, we can approximate $\mathrm{y}_{f,0,t}(w_t, \cdot, m_{h,t})$ by first setting an exogenous grid (over the constrained and unconstrained regions) of $y_{f,t}$ and c_t values (holding $y_{h,t} = m_{h,t}$ fixed as no adjustment occurs), and then creating an endogenous grid of time t financial assets $m_{f,t}$ using (24) and budget constraint (23). RFC algorithm can then be applied to eliminate sub-optimal points.

The *adjuster's* Bellman equation implies their solution only depends on total resources $\bar{m}_t = m_{f,t} + m_{h,t}$. Thus, the dimension of the active state space $\mathbb{R}_+$ (one) is less than the dimensions of the post-states (two). There will then be multiple one-dimensional submanifolds embedded in the post-state space from which the adjuster Euler equations can be inverted. The submanifolds will be characterized by financial and housing asset values that satisfy Euler equation (25). To construct the exogenous grid, we start with a regular grid of $y_{h,t}$ values. Note we can evaluate time t consumption c_t, given the values of $y_{h,t}$ and $y_{f,t}$, as $c_t = \partial_c \mathrm{v}^{-1}((1+r)\beta \lambda_{f,t+1}(m_{f,t+1}, m_{h,t+1}), y_{h,t})$, where $\partial_c \mathrm{v}^{-1}$ is the analytical inverse of $\partial_c \mathrm{v}$ in its first argument. By plugging c_t into (25), for each $y^{\#}_{h,t}$ we can evaluate the multiple roots of (25) in terms of $y_{f,t}$ to form an irregular exogenous grid. The pseudocode to approximate the adjuster policy functions is detailed in the online appendix H.2.

Finally, note that the endogenous grid points $\mathcal{M}_t$ will not be monotone in end-of-period housing - see Figure (4). This is because as agents become wealthier, they will reach a threshold where they anticipate upgrading their housing stock sometimes in the future. At this threshold, they also expect to discontinuously decrease future non-housing consumption, causing a jump up in the RHS of (25). As a result, they will discontinuously decrease current period housing consumption. Moreover, the optimal housing policy that takes into account the future sequence of adjustment decisions will be non-monotone. This means existing upper-envelope methods (Fella, 2014; Iskhakov et al., 2017; Druedahl and Jørgensen, 2017) cannot be applied. As discussed in Section 6.1, however, we can implement RFC by setting $\bar{J} = 1$ and $\rho_r > \frac{2\epsilon}{\underline{\mathrm{MPC}}}$, and

also set end-of-period housing $a \mapsto \hat{y}_{h,t}(a)$ and consumption $a \mapsto \hat{c}_t(a)$ as the grid pasting function κ_t for adjusters and non-adjusters, respectively.

Numerical implementation. To parameterize the model, we set $\rho = 3$, $\alpha = 0.66$, $\beta = .93$, $\tau = .18$, $r = 0.01$, and $T = 60$. We assume $\tilde{w}_t$ is the earnings function for females in Dobrescu et al. (2018), with $w_t = \tilde{w}_t(\tilde{z})$ and $\tilde{\eta}$ being a random variable taking values in $\{0.1, 1\}$ with equal probability; for simplicity, earnings shocks are i.i.d . To benchmark our method with the others, we implement the solution algorithm using VFI, EGM with RFC, and the NEGM method in Druedahl (2021). As the financial assets and total resources grids are one-dimensional, we use standard linear interpolation to implement all methods.

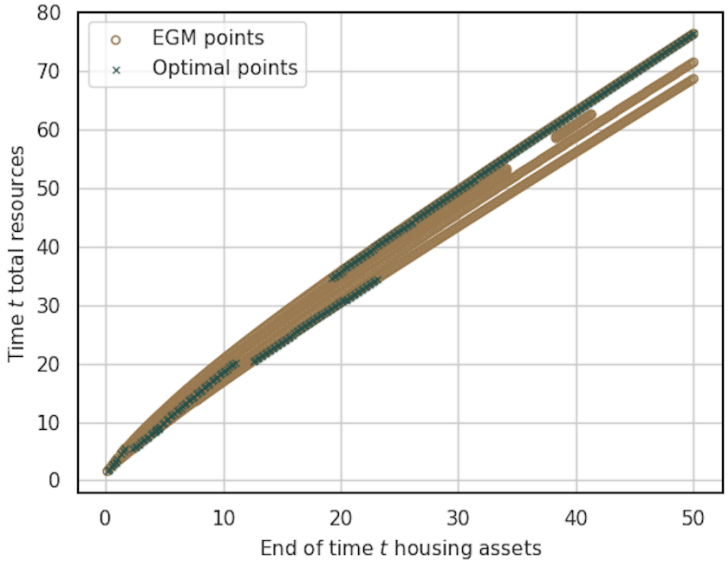

FIGURE 4. Endogenous total resources on an exogenous grid

Figure 4 shows the map of endogenous grid points to the exogenous grid for a 59 year old, with the exogenous grid points belonging to a subset of a collection of one-dimensional spaces, each corresponding to a particular future sequence of discrete choices. Despite the irregular grid and non-monotonicity of the optimal policy, we see that the RFC recovers the optimal points. Finally, the left panel of Figure 5 compares computational speed across methods, and shows that despite the intermediate root-finding step, EGM with RFC (i) still outperforms VFI by a factor of more than 20, and (ii) is comparable in scale with NEGM but still 25% faster. As expected, since EGM with root finding uses all the information contained in the Euler equation to compute the optimal policy, the right panel of Figure 5 shows that our RFC algorithm delivers up to an order of magnitude improvement in accuracy over both VFI and NEGM.

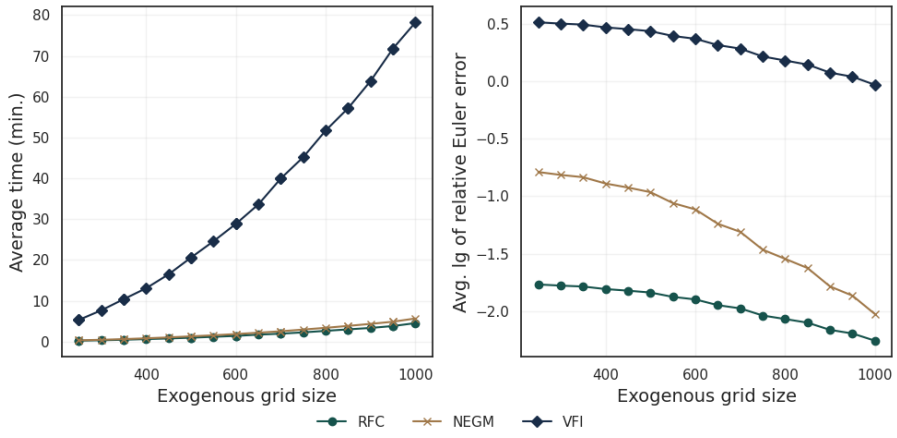

FIGURE 5. Computational speed and Euler error benchmarking

7. Conclusions

This study resolves several critical challenges in applying dynamic programming methods to solve multidimensional stochastic optimization models with discrete-continuous choices and occasionally binding constraints. Our contribution enables a rigorous and systematic implementation of the inverse Euler equation to maximize the use of first order information to solve such models efficiently. In particular, by introducing the S-function, we establish a general (and painless) way to derive the necessary Euler equation in all classes of models with non-compact feasibility correspondences, unbounded rewards, occasionally binding constraints, and discrete choices. We are also the first to provide verifiable conditions on the model primitives that determine when the inverse Euler equation is well-defined. Additionally, our RFC algorithm offers a highly efficient and accurate avenue to solve discrete-continuous problems. This algorithm is not only compatible with vectorized, high-performance computing but also introduces verifiable error bounds for the inverse Euler equation methods applied to models *with and without* discrete choices. We demonstrate the practical impact of our contributions via two workhorse applications, with a special focus on our method's ability to handle multidimensional problems that could not be previously solved with EGM, and the RFC gains in computational speed and accuracy.

Appendix A. Proofs for Section 3

A.1. **Preliminaries.** In this appendix, bold italic letters denote abstract vectors and bold italic capital letters denote abstract vector spaces. Moreover, let $\{\mathscr{F}_t\}_{t=0}^T$ denote the natural filtration of $\{w_t\}_{t=0}^T$.

Definition 2. ***(Integral operator)*** *Let* $(\Omega, \Sigma, \mathbb{P})$ *be a probability space,* $\boldsymbol{X} = L^2(\Omega, \mathbb{R}^N, \Sigma)$*, and* $\mathrm{f}\colon \mathbb{R}^N \times \mathbb{R}^K \to \bar{\mathbb{R}}$*. For* $\boldsymbol{y} \in L^2(\Omega, \mathbb{R}^K, \Sigma)$*, the integral operator with kernel* f *is* $\mathrm{I}_\mathrm{f}\colon \boldsymbol{X} \to \bar{\mathbb{R}}$ *defined by the evaluation* $\mathrm{I}_\mathrm{f}(\boldsymbol{x}) = \int \mathrm{f}(\boldsymbol{x}(\omega), \boldsymbol{y}(\omega))\mathbb{P}(d\omega)$.

In what follows, $\partial^S \mathrm{f}$ is the supdifferential of a function f (see online appendix D.2).

Proposition A.1. *(**Supdifferential of integral operator**) If $\boldsymbol{\phi} \in \partial^S_{\boldsymbol{x}} \mathrm{I}_{\mathrm{f}}(\boldsymbol{x})$ for $\boldsymbol{x} \in \operatorname{dom} \mathrm{f}$ and $\partial_x \mathrm{f}(\boldsymbol{x}(\omega), \boldsymbol{y}(\omega))$ is defined for ω a.e., then $\boldsymbol{\phi} = \partial_x \mathrm{f}(\boldsymbol{x}, \boldsymbol{y})$ a.e.*

Proof. By the definition of a supderivative, $\boldsymbol{\phi}(\boldsymbol{s}-\boldsymbol{x}) \geq \mathrm{f}(\boldsymbol{s}, \boldsymbol{y}) - \mathrm{f}(\boldsymbol{x}, \boldsymbol{y})$ a.e. for all $\boldsymbol{s} \in \boldsymbol{X}$ (see online appendix Claim D.1.) Thus, $\boldsymbol{\phi}(\omega)$ is a.e. a supdifferential of $\mathrm{f}(\cdot, \boldsymbol{y}(\omega))$. Since $\mathrm{f}(\cdot, \boldsymbol{y}(\omega))$ is concave and differentiable, its supdifferential at $\boldsymbol{x}(\omega)$ is uniquely given by $\partial_x \mathrm{f}(\boldsymbol{x}(\omega), \boldsymbol{y}(\omega))$. As such, $\boldsymbol{\phi}(\omega) = \partial_x \mathrm{f}(\boldsymbol{x}(\omega), \boldsymbol{y}(\omega))$ for ω a.e. □

A.2. **Hilbert space dynamic optimization problem.** The Hilbert space problem consists of the following for each t:

(1) $\boldsymbol{X}_t = \boldsymbol{W}_t \times \boldsymbol{Z}_t \times \boldsymbol{M}_t$ s.t. $\boldsymbol{W}_t \subset L^2\left(\Omega, \mathbb{R}^{N_W}, \mathscr{F}_t\right)$, $\boldsymbol{Z}_t \subset L^2\left(\Omega, \mathbb{R}^{N_Z}, \mathscr{F}_t\right)$, and $\boldsymbol{M}_t \subset L^2\left(\Omega, \mathbb{R}^{N_M}, \mathscr{F}_t\right)$.
(2) $\boldsymbol{D}_t \times \boldsymbol{Y}_t$ s.t. $\boldsymbol{D}_t \subset L^2\left(\Omega, \mathbb{N}^{N_D}, \mathscr{F}_t\right)$, and $\boldsymbol{Y}_t \subset L^2\left(\Omega, \mathbb{R}^{N_Y}, \mathscr{F}_t\right)$,
(3) $\vec{\boldsymbol{\Gamma}}_t$ with $\vec{\boldsymbol{\Gamma}}_t \colon \boldsymbol{X}_t \rightrightarrows \boldsymbol{D}_t \times \boldsymbol{Y}_t$ s.t. $\boldsymbol{d}_t, \boldsymbol{y}_t \in \vec{\boldsymbol{\Gamma}}_t(\boldsymbol{x}_t,)$ iff $\mathbf{g}_t(\boldsymbol{w}_t, \boldsymbol{z}_t, \boldsymbol{m}_t, \boldsymbol{d}_t, \boldsymbol{y}_t) \geq 0$,
(4) $\mathbf{u}_t$ with $\mathbf{u}_t \colon \mathrm{Gr}\vec{\boldsymbol{\Gamma}}_t \to \mathbb{R} \cup \{-\infty\}$,
(5) $\mathbf{F}^m_t$ s.t. $\mathbf{F}^m_t \colon \boldsymbol{D}_t \times \boldsymbol{Y}_t \times \boldsymbol{W}_{t+1} \to \boldsymbol{M}_{t+1}$, and $\mathbf{F}^d_t$, with $\mathbf{F}^d_t \colon \boldsymbol{D}_t \times \boldsymbol{W}_{t+1} \to \boldsymbol{Z}_{t+1}$.

Let $\mathbf{F}_t \colon = (\mathrm{F}^w_t, \mathbf{F}^m_t, \mathbf{F}^d_t)$, $\mathbf{u}_t(\boldsymbol{w}_t, \boldsymbol{z}_t, \boldsymbol{m}_t, \boldsymbol{d}_t) = \mathbb{E}_0 \mathrm{u}_t(\boldsymbol{w}_t, \boldsymbol{z}_t, \boldsymbol{m}_t, \boldsymbol{d}_t)$, $\mathbf{g}_t(\boldsymbol{w}_t, \boldsymbol{z}_t \boldsymbol{m}_t, \boldsymbol{d}_t, \boldsymbol{y}_t) = \mathrm{g}_t(\boldsymbol{w}_t, \boldsymbol{z}_t, \boldsymbol{m}_t, \boldsymbol{d}_t, \boldsymbol{y}_t)$, and $\boldsymbol{x}_{t+1}, = \mathbf{F}_t(\boldsymbol{d}_t, \boldsymbol{y}_t, \boldsymbol{w}_{t+1}) = \mathrm{F}_t(\boldsymbol{d}_t, \boldsymbol{y}_t, \boldsymbol{w}_{t+1})$ a.e., $\forall\, t$. We then have

$$\textbf{(DV)} \qquad \mathbf{v}_0(\boldsymbol{x}_0) \colon = \max_{\{\boldsymbol{x}_t, \boldsymbol{d}_t, \boldsymbol{y}_t\}_{t=0}^T} \left[\sum_{t=0}^T \mathbf{u}_t(\boldsymbol{x}_t, \boldsymbol{d}_t, \boldsymbol{y}_t) \right], \qquad \boldsymbol{x}_0 \in \boldsymbol{X}_0$$

s.t. $\forall\, t$, $\boldsymbol{x}_t, \in \boldsymbol{X}_t$, $\boldsymbol{d}_t \in \boldsymbol{D}_t$, $\boldsymbol{y}_t \in \boldsymbol{Y}_t$, $\boldsymbol{d}_t, \boldsymbol{y}_t \in \vec{\boldsymbol{\Gamma}}_t(\boldsymbol{x}_t)$, and $\boldsymbol{x}_{t+1}, = \mathrm{F}_t(\boldsymbol{d}_t, \boldsymbol{y}_t, \boldsymbol{w}_{t+1})$. We also define

$$\textbf{(CS-DV)} \qquad \mathbf{v}_0^{\vec{\boldsymbol{d}}_0}(\boldsymbol{x}_0) \colon = \max_{\{\boldsymbol{x}_t, \boldsymbol{y}_t\}_{t=0}^T} \sum_{t=0}^T \mathbf{u}_t(\boldsymbol{w}_t, \boldsymbol{z}_t, \boldsymbol{m}_t, \boldsymbol{d}_t, \boldsymbol{y}_t), \qquad \boldsymbol{x}_0 \in \boldsymbol{X}_0$$

s.t. $\{\boldsymbol{x}_t, \boldsymbol{y}_t\}_{t=0}^T$ is feasible, and $\vec{\boldsymbol{d}}_0 = \{\boldsymbol{d}_0, \ldots, \boldsymbol{d}_T\}$.

A.3. **Necessity of generalized Euler equation.**

Proposition A.2. *If Assumptions 2.1, 3.1 and 3.2 hold, and $\{\boldsymbol{x}_t, \boldsymbol{d}_t, \boldsymbol{y}_t\}_{t=0}^T$ is generated by policy functions $\{\mathrm{y}_t, \mathrm{d}\}_{t=0}^T$, then $\exists$ $\{\boldsymbol{\mu}_t, \boldsymbol{\lambda}_{t+1}\}_{t=0}^T$ s.t., $\boldsymbol{\lambda}_{t+1} \in L^2\left(\Omega, \mathbb{R}^{N_M}, \mathscr{F}_t\right)$, $\boldsymbol{\mu}_t \in L^2\left(\Omega, \mathbb{R}^{N_g}, \mathscr{F}_t\right)$, and*

$$\partial_y \mathrm{u}_t(\boldsymbol{x}_t, \boldsymbol{d}_t, \boldsymbol{y}_t) + \boldsymbol{\mu}_t^\top \partial_y \mathrm{g}_t(\boldsymbol{x}_t, \boldsymbol{d}_t, \boldsymbol{y}_t) + \mathbb{E}_t \boldsymbol{\lambda}_{t+1}^\top \partial_y \mathrm{F}^m(\boldsymbol{w}_t, \boldsymbol{d}_t, \boldsymbol{y}_t) = \mathbf{0}, \tag{26}$$

$$\partial_m \mathrm{u}_{t+1}(\boldsymbol{x}_{t+1}, \boldsymbol{d}_{t+1}, \boldsymbol{y}_{t+1}) + \boldsymbol{\mu}_{t+1}^\top \partial_m \mathrm{g}_{t+1}(\boldsymbol{x}_{t+1}, \boldsymbol{d}_{t+1}, \boldsymbol{y}_{t+1}) - \boldsymbol{\lambda}_{t+1}^\top = \mathbf{0}, \tag{27}$$

$$\boldsymbol{\mu}_{t+1} \circ \mathrm{g}_{t+1}(\boldsymbol{x}_{t+1}, \boldsymbol{d}_{t+1}, \boldsymbol{y}_{t+1}) = 0. \tag{28}$$

Proof. If $\{\boldsymbol{x}_t, \boldsymbol{d}_t, \boldsymbol{y}_t\}_{t=0}^T$ is generated by $\{\mathrm{y}_t, \mathrm{d}\}_{t=0}^T$, then $\{\boldsymbol{x}_t, \boldsymbol{y}_t\}_{t=0}^T$ solves problem (**CS-DV**) given $\vec{\boldsymbol{d}}_0 = \{\boldsymbol{d}_t\}_{t=0}^T$. As such, $\{\boldsymbol{y}_t, \boldsymbol{m}_{t+1}\}$ solves the following one-shot problem:

$$\max_{\boldsymbol{y}, \boldsymbol{m}'} \quad \mathbf{u}_t(\boldsymbol{x}_t, \boldsymbol{d}_t, \boldsymbol{y}) + \mathbf{u}_{t+1}(\boldsymbol{w}_{t+1}, \boldsymbol{z}_{t+1}, \boldsymbol{m}', \boldsymbol{d}_{t+1}, \boldsymbol{y}') =: U_t(\boldsymbol{y}, \boldsymbol{m}_{t+1}), \qquad \forall t$$

subject to $\boldsymbol{y} \in \boldsymbol{Y}_t$, $\boldsymbol{m}' \in \boldsymbol{M}_{t+1}$, $\mathbf{g}_t(\boldsymbol{w}_t, \boldsymbol{z}_t, \boldsymbol{m}_t, \boldsymbol{d}_t, \boldsymbol{y}) \geq \mathbf{0}$, $\mathbf{F}_t^m(\boldsymbol{d}_t, \boldsymbol{y}, \boldsymbol{w}_{t+1}) - \boldsymbol{m}' = \mathbf{0}$, and $\mathbf{g}_{t+1}(\boldsymbol{w}_{t+1}, \boldsymbol{z}_{t+1}, \boldsymbol{m}', \boldsymbol{d}_{t+1}, \boldsymbol{y}_{t+1}) \geq \mathbf{0}$. By the constraint qualification implied in Assumption 3.3, and applying Fermat's theorem (see online appendix Theorem D.1), there exists $\boldsymbol{\mu}_t \in L^2\left(\Omega, \mathbb{R}^{N_g}, \mathscr{F}_t\right)$, $\boldsymbol{\mu}_{t+1} \in L^2\left(\Omega, \mathbb{R}^{N_g}, \mathscr{F}_{t+1}\right)$, and $\boldsymbol{\lambda}_{t+1} \in L^2\left(\Omega, \mathbb{R}^{N_M}, \mathscr{F}_{t+1}\right)$ such that (28) holds (see, for instance, Theorem 2 in (Wachsmuth, 2013)) and

$$\mathbf{0} \in \partial^S_{(\boldsymbol{y}, \boldsymbol{m}')} \big\{ U_t(\boldsymbol{y}_{t+1}, \boldsymbol{m}_{t+1}) + \boldsymbol{\mu}_t \mathbf{g}_t(\boldsymbol{x}_t, \boldsymbol{d}_t, \boldsymbol{y}_t) + \boldsymbol{\lambda}_{t+1}\left(\mathbf{F}_t^m(\boldsymbol{d}_t, \boldsymbol{y}_t, \boldsymbol{w}_{t+1}) - \boldsymbol{m}_{t+1}\right) + \boldsymbol{\mu}_{t+1}\mathbf{g}_{t+1}(\boldsymbol{x}_{t+1}, \boldsymbol{d}_{t+1}, \boldsymbol{y}_{t+1}) \big\}, \qquad \forall\, t.$$

Taking partial supderivatives (see online appendix Fact 1) with respect to $\boldsymbol{y}$ and $\boldsymbol{m}'$:

$$\begin{aligned} \mathbf{0} &\in \partial^S_{\boldsymbol{y}} \left\{ \mathbf{u}_t(\boldsymbol{x}_t, \boldsymbol{d}_t, \boldsymbol{y}_t) + \boldsymbol{\mu}_t \mathbf{g}_t(\boldsymbol{x}_t, \boldsymbol{d}_t, \boldsymbol{y}_t) + \boldsymbol{\lambda}_{t+1}\mathbf{F}_t^m(\boldsymbol{d}_t, \boldsymbol{y}_t, \boldsymbol{w}_{t+1}) \right\}, \\ \mathbf{0} &\in \partial^S_{\boldsymbol{m}} \left\{ \mathbf{u}_{t+1}(\boldsymbol{x}_{t+1}, \boldsymbol{d}_{t+1}, \boldsymbol{y}_{t+1}) + \boldsymbol{\mu}_{t+1}\mathbf{g}_{t+1}(\boldsymbol{x}_{t+1}, \boldsymbol{d}_{t+1}, \boldsymbol{y}_{t+1}) - \boldsymbol{\lambda}_{t+1}\boldsymbol{m}_t \right\}. \end{aligned}$$

Let $\boldsymbol{y} \mapsto \mathbf{u}_t(\boldsymbol{x}_t, \boldsymbol{d}_t, \boldsymbol{y}) + \boldsymbol{\mu}_t \mathbf{g}_t(\boldsymbol{x}_t, \boldsymbol{d}_t, \boldsymbol{y}) + \boldsymbol{\lambda}_{t+1}\mathbf{F}_t^m(\boldsymbol{d}_t, \boldsymbol{y}, \boldsymbol{w}_{t+1})$ be an integral operator (see Definition 2) with kernel $\mathbf{S}_t(\boldsymbol{m}_t, \cdot, \boldsymbol{\mu}_t, \mathbf{0} \,|\, \boldsymbol{\lambda}')$ as follows:

$$\begin{aligned} \mathrm{I}_{\mathbf{S}_t(\boldsymbol{m}_t, \cdot, \boldsymbol{\mu}_t, \mathbf{0} \,|\, \lambda')}(\boldsymbol{m}, \boldsymbol{y}) &= \int \mathbf{S}_t(\boldsymbol{m}_t(\omega), \boldsymbol{y}(\omega), \boldsymbol{\mu}_t(\omega), \mathbf{0} \,|\, \boldsymbol{\lambda}'(\omega))\, \mathbb{P}(\mathrm{d}\omega) \\ &= \mathbf{u}_t(\boldsymbol{w}_t, \boldsymbol{z}_t, \boldsymbol{d}_t, \boldsymbol{m}_t, \boldsymbol{y}) + \mathbb{E}_t \boldsymbol{\lambda}_{t+1}\mathbf{F}_t^m(\boldsymbol{d}_t, \boldsymbol{y}, \boldsymbol{w}_{t+1}) + \boldsymbol{\mu}_t \mathbf{g}_t(\boldsymbol{w}_t, \boldsymbol{z}_t, \boldsymbol{m}_t, \boldsymbol{y}), \quad \boldsymbol{\lambda}' = \mathbb{E}_t \boldsymbol{\lambda}_{t+1}. \end{aligned}$$

Since $\partial_y \mathbf{S}_t(\boldsymbol{m}_t, \boldsymbol{y}_t, \boldsymbol{\mu}_t, \mathbf{0} \,|\, \boldsymbol{\lambda}')$ exists a.e. by Assumption 3.1, and since $\mathbf{S}_t(\boldsymbol{m}_t, \cdot, \boldsymbol{\mu}_t, \mathbf{0} \,|\, \boldsymbol{\lambda}')$ is concave, apply Proposition A.1 to arrive at (27). Similarly, $\partial_m \mathbf{S}_{t+1}(\boldsymbol{m}_{t+1}, \boldsymbol{y}_{t+1}, \boldsymbol{\mu}_{t+1} \,|\, \boldsymbol{\lambda}'')$ exists a.e., and $\mathbf{S}_{t+1}(\cdot, \boldsymbol{y}_t, \boldsymbol{\mu}_{t+1}, \boldsymbol{\lambda}_{t+1} \,|\, \boldsymbol{\lambda}')$ is concave. Thus, by Proposition A.1, (28) holds. □

Proof of Theorem 3.1. We show for $\forall t$, $\exists$ measurable μ_t and λ_{t+1} such that

$$\partial_y \mathrm{u}_t(\boldsymbol{x}_t, \boldsymbol{d}_t, \boldsymbol{y}_t) + \mu_t(\boldsymbol{x}_t)^\top \partial_y \mathrm{g}_t(\boldsymbol{x}_t, \boldsymbol{d}_t, \boldsymbol{y}_t) + \mathbb{E}_t \lambda_{t+1}(\boldsymbol{x}_t,)^\top \partial_y \mathrm{F}^m(\boldsymbol{w}_t, \boldsymbol{d}_t, \boldsymbol{y}_t) = \mathbf{0} \tag{29}$$

$$\partial_{\boldsymbol{m}} \mathrm{u}_{t+1}(\boldsymbol{x}_{t+1}, \boldsymbol{d}_{t+1}, \boldsymbol{y}_{t+1}) + \mu_t(\boldsymbol{x}_t)^\top \partial_{\boldsymbol{m}} \mathrm{g}_{t+1}(\boldsymbol{x}_{t+1}, \boldsymbol{d}_{t+1}, \boldsymbol{y}_{t+1}) - \lambda_{t+1}(\boldsymbol{x}_t)^\top = \mathbf{0} \tag{30}$$

Define $\tilde{\mu}_t := \mathbb{E}(\mu_t \,|\, x_t)$ and $\tilde{\lambda}_{t+1} := \mathbb{E}(\lambda_t \,|\, x_{t+1})$. From (26), and using the tower property,

$$\mathbb{E}\Big[\partial_y \mathrm{u}_t(\boldsymbol{x}_t, \boldsymbol{d}_t, \boldsymbol{y}_t) + \mu_t^\top \partial_y \mathrm{g}_t(\boldsymbol{x}_t, \boldsymbol{d}_t, \boldsymbol{y}_t) + \mathbb{E}\left[\lambda_{t+1}^\top \partial_y \mathrm{F}^m(\boldsymbol{w}_t, \boldsymbol{d}_t, \boldsymbol{y}_t) \,|\, x_{t+1} \right] \Big| x_t \Big] = \mathbf{0}.$$

Pulling out known factors, $\partial_y \mathrm{u}_t(\boldsymbol{x}_t, \boldsymbol{d}_t, \boldsymbol{y}_t) + \tilde{\mu}_t^\top \partial_y \mathrm{g}_t(\boldsymbol{x}_t, \boldsymbol{d}_t, \boldsymbol{y}_t) + \mathbb{E}_t \tilde{\lambda}_{t+1}^\top \partial_y \mathrm{F}_t^m(\boldsymbol{w}_t, \boldsymbol{d}_t, \boldsymbol{y}_t) = \mathbf{0}$. Similarly, by (27), $\partial_{\boldsymbol{m}} \mathrm{u}_{t+1}(\boldsymbol{x}_{t+1}, \boldsymbol{d}_{t+1}, \boldsymbol{y}_{t+1}) + \tilde{\mu}_{t+1}^\top \partial_{\boldsymbol{m}} \mathrm{g}_{t+1}(\boldsymbol{x}_{t+1}, \boldsymbol{d}_{t+1}, \boldsymbol{y}_{t+1}) - \tilde{\lambda}_{t+1}^\top = \mathbf{0}$. Since $\tilde{\mu}_t$ is x_t-measurable and $\tilde{\lambda}_{t+1}$ is x_{t+1}-measurable, $\exists$ μ_t and λ_{t+1} s.t. (29)-(30) hold. □

Appendix B. Proofs for Section 4

Proof of Theorem 4.1. Consider the mapping $\Psi\colon \bar{M}_t^{\mathrm{o}} \times \left(\pi_{\tilde{A}} K_{l,t}\right)^{\mathrm{o}} \to \mathbb{R}^{N_{\bar{M}}}$ given by $\bar{m}, \tilde{a} \mapsto \pi_{N_Y} \bar{\mathbf{E}}_t(\bar{m}, \mathrm{em}_{\tilde{A}}(\tilde{a}))$ where $M_t{}^{\mathrm{o}}$ and $\left(\pi_{\tilde{A}} K_{l,t}\right)^{\mathrm{o}}$ are both open sets in $\mathbb{R}^{N_{\bar{M}}}$. Note that $\Psi(\cdot, \tilde{a})$ is injective for each $\tilde{a} \in \left(\pi_{\tilde{A}} K_{l,t}\right)^{\mathrm{o}}$ by (6). Moreover, $\lambda_{t+1}^{\vec{d}_t}$ is continuous in m_{t+1} by Assumption 3.3 (see online appendix Lemma E.1). Thus, by the implicit function theorem (Theorem 1.1. in Kumagai (1980)), there exists an open neighborhood $U_{0,\bar{m}}$ of $\bar{m}_t$, an open neighborhood $U_{0,\tilde{a}}$ of $\tilde{a}_t$, and a continuous function φ_0 such that for each $\tilde{a} \in U_{0,\tilde{a}}$, $\varphi_0(\tilde{a}) \in U_{0,\bar{m}}$, and $\Psi(\varphi_0(\tilde{a}), \tilde{a}) = 0$. Next, let $\bar{\mathrm{g}}_t^l$ be the set of binding constraint functions in the region l. By Assumption 3.3, $\partial_y \bar{\mathrm{g}}_t^l(\bar{m}, y)^\top$ is invertible for $\bar{m}, y \in K_{l,t}$. Define

$$\hat{\mu}\colon = -\left(\partial_{\hat{y}} \bar{\mathrm{g}}_t^l(\bar{m}, y)^\top\right)^{-1} \left[\mathbb{E}_{w_t} \lambda_{t+1}(x')^\top \partial_{\hat{y}} \mathrm{F}_{t+1}^m \left(d_t, \pi_Y \mathrm{em}_{\tilde{A}} \tilde{a}, w_{t+1}\right) + \partial_{\hat{y}} \bar{\mathrm{u}}(\varphi_0(\tilde{a}), \pi_Y \mathrm{em}_{\tilde{A}} \tilde{a})\right], \tag{31}$$

with $x' = \mathrm{F}(d_t, \pi_Y \mathrm{em}_{\tilde{A}} \tilde{a}, w_{t+1})$, and $\hat{y}$ the post-states such that $\partial_{y_i} \bar{\mathrm{g}}_t^l(\bar{m}, y) \neq 0$. The vector $\hat{\mu}$ will be the multipliers associated with N^l binding constraints. For all i s.t $\partial_{y_i} \bar{\mathrm{g}}_t^l(\bar{m}, y) \neq 0$,

$$\partial_{y_i} \bar{\mathrm{u}}(\varphi(\tilde{a}), \pi_Y \mathrm{em}_{\tilde{A}} \tilde{a}) + \hat{\mu}^\top \partial_{y_i} \bar{\mathrm{g}}_t(\bar{m}, y) + \mathbb{E}_{w_t} \lambda_{t+1}(x')^\top \partial_{y_i} \mathrm{F}_{t+1}^m \left(d_t, \pi_Y \mathrm{em}_{\tilde{A}} \tilde{a}, w_{t+1}\right) = 0. \tag{32}$$

Next, since $\varphi_0(\tilde{a}) \in U_{0,\bar{m}}$, and $\Psi(\varphi_0(\tilde{a}), \tilde{a}) = 0$ for i such that $\partial_{y_i} \bar{\mathrm{g}}_t^l(\bar{m}, y) = 0$,

$$\partial_{y_i} \bar{\mathrm{u}}(\varphi(\tilde{a}), \pi_Y \mathrm{em}_{\tilde{A}} \tilde{a}) + \mathbb{E}_{w_t} \partial_{y_i} \lambda_{t+1}(x')^\top \partial_{y_i} \mathrm{F}_{t+1}^m \left(d_t, \pi_Y \mathrm{em}_{\tilde{A}} \tilde{a}, w_{t+1}\right) = 0. \tag{33}$$

Moreover, since $\left(\varphi(\tilde{a}), \pi_Y \mathrm{em}_{\tilde{A}} \tilde{a}\right) \in K_{l,t}$, $\bar{\mathrm{g}}_t^l(\varphi(\tilde{a}), \pi_Y \mathrm{em}_{\tilde{A}} \tilde{a}) \geq 0$. Finally, let φ be defined by $\tilde{a} \mapsto \mu, \pi_Y \mathrm{em}_{\tilde{A}} \tilde{a}$, where μ is obtained by permutation of indices of vectors in $[\hat{\mu}, \mathbf{0}_{N_g - N^l}]$, and $\mathbf{0}_{N_g - N^l}$ is the value of the multipliers for the non-binding constraints. To complete the proof, note that since (32)-(33) also hold, we must have $\bar{\mathbf{E}}_t(\varphi_0(\tilde{a}), \varphi(\tilde{a})) = 0$ for each $\tilde{a} \in U_{0,\tilde{a}}$ and s.t. $(\varphi_0(\tilde{a}), \varphi(\tilde{a})) \in K_{l,t}$. □

Appendix C. Proofs for Section 5

Proposition C.1. *Let the conditions of Theorem 5.1 hold. For $\bar{m} \in \bar{M}_t$ a.e., $\exists\ \bar{N}$ s.t. if $\bar{m}_{t,i}^{\#} \in \mathbb{B}_{L_2 \epsilon_{|\mathcal{A}_t|}}(\bar{m}) \cap \mathcal{M}_t^{\mathrm{RFC}}$, then $\|\kappa_t(\sigma_t(\bar{m}_{t,i}^{\#})) - \kappa_t(a_{t,i}^{\#})\| < C_0 L_1 L_2 \epsilon_{|\mathcal{A}_t|}$ for all $|\mathcal{A}_t| > \bar{N}$.*

Proof. For any $\bar{m} \in \bar{M}_t$ a.e., $\exists\ \bar{\delta}$ s.t. $\boldsymbol{d}_{t+1}$ is the optimal sequence of future discrete choices for any $\bar{m}_{t,i}^{\#} \in \mathbb{B}_{\bar{\delta}}(\bar{m})$ (see online appendix Lemma G.1). Next, by Assumptions 5.2 and 5.3, $\exists\ \bar{m}_{t,k^\star}^{\#}$ with $\bar{m}_{t,k^\star}^{\#} \in \mathbb{B}_{\bar{\delta}}(\bar{m})$ s.t. $a_{t,k^\star}^{\#}$ is optimal given $\bar{m}_{t,k^\star}^{\#}$. Moreover, we can set $\bar{N}$ large enough s.t. for any $\bar{m}_{t,i}^{\#} \in \mathbb{B}_{L_2 \epsilon_{|\mathcal{A}_t|}}(\bar{m})$, $\|\bar{m}_{t,i}^{\#} - \bar{m}_{t,k^\star}^{\#}\| \leq C_0 L_2 \epsilon_{|\mathcal{A}_t|}$ and we have that $\bar{m}_{t,k^\star}^{\#} \in \mathbb{B}_{\epsilon_{|\mathcal{A}_t|}}(\bar{m})$ s.t. $a_{t,k^\star}^{\#}$ is optimal given $\bar{m}_{t,k^\star}^{\#}$. Suppose for some $\bar{m}_{t,i}^{\#} \in \mathbb{B}_{L_2 \epsilon_{|\mathcal{A}_t|}}(\bar{m})$, $\hat{\vec{\boldsymbol{d}}}_{t+1}$ is s.t. $a_{t,i}^{\#} = \sigma_t^{\hat{\vec{\boldsymbol{d}}}_{t+1}}(\bar{m}_{t,i}^{\#})$ and $\hat{\vec{\boldsymbol{d}}}_{t+1} \neq \vec{\boldsymbol{d}}_{t+1}$. Since $C_0 L_2 \epsilon_{|\mathcal{A}_t|} \leq \rho_r$

and $\bar{m}^{\#}_{t,i} \in \mathcal{M}^{\text{RFC}}_t$, we have $\|\bar{m}^{\#}_{t,i} - \bar{m}^{\#}_{t,k^\star}\| \leq \rho_r$ (see Box 1). Next, let $\underline{\kappa} = \|\kappa_t(\sigma_t(\bar{m}^{\#}_{t,i})) - \kappa_t(\sigma_t^{\hat{\vec{d}}_{t+1}}(\bar{m}^{\#}_{t,i}))\|$,

$$\begin{aligned}\|\kappa_t(\sigma_t^{\vec{d}_{t+1}}(\bar{m}^{\#}_{t,k^\star})) - \kappa_t(\sigma_t^{\hat{\vec{d}}_{t+1}}(\bar{m}^{\#}_{t,i}))\| \geq \Big| &\|\kappa_t(\sigma_t^{\boldsymbol{d}_{t+1}}(\bar{m}^{\#}_{t,i})) - \kappa_t(\sigma_t^{\hat{\vec{d}}_{t+1}}(\bar{m}^{\#}_{t,i}))\| \\ &- \|\kappa_t(\sigma_t^{\vec{d}_{t+1}}(\bar{m}^{\#}_{t,i})) - \kappa_t(\sigma_t^{\vec{d}_{t+1}}(\bar{m}^{\#}_{t,k^\star}))\|\Big| \\ &\geq |\underline{\kappa} - \epsilon_{|\mathcal{A}_t|}|.\end{aligned}$$

Letting $\underline{\kappa} > \epsilon_{|\mathcal{A}_t|}$, and $\frac{\underline{\kappa}}{\|\bar{m}^{\#}_{t,i} - \bar{m}^{\#}_{t,k^\star}\|} < \frac{\|\kappa_t(\sigma_t^{\vec{d}_{t+1}}(\bar{m}^{\#}_{t,k^\star})) - \kappa_t(\sigma_t^{\hat{\vec{d}}_{t+1}}(\bar{m}^{\#}_{t,i}))\| + L_2 L_1 \epsilon_{|\mathcal{A}_t|}}{\|\bar{m}^{\#}_{t,i} - \bar{m}^{\#}_{t,k^\star}\|} < \bar{J} + \frac{\epsilon_{|\mathcal{A}_t|}}{\|\bar{m}^{\#}_{t,i} - \bar{m}^{\#}_{t,k^\star}\|}$, we can conclude $\underline{\kappa} < \bar{J} C_0 L_2 \epsilon_{|\mathcal{A}_t|} + \epsilon_{|\mathcal{A}_t|}$. □

Proof of Theorem 5.1. For any $\bar{m} \in \bar{M}_t$ a.e., $\exists\ \delta > 0$ s.t. $\boldsymbol{d}_{t+1}$ is the optimal sequence of future discrete choices for any $\bar{m}^{\#}_{t,i} \in \mathbb{B}_\delta(\bar{m})$ (see online appendix Lemma G.1). Moreover, by Proposition C.1, there exists $|\mathcal{A}_t|$ large enough s.t. $\|\kappa_t(\sigma_t(\bar{m}^{\#}_{t,i})) - \kappa_t(a^{\#}_{t,i})\| < C_0 L_1 L_2 \epsilon_{|\mathcal{A}_t|} + \epsilon_{|\mathcal{A}_t|}$ for any $\bar{m}^{\#}_{t,i} \in \mathbb{B}_{L_2\epsilon_{|\mathcal{A}_t|}}(\bar{m})$. We have three cases. First consider the case when $D_t = 1$ for all t. If there does not exist $N_{\bar{M}} + 1$ vertices of a simplex completely contained in $\mathbb{B}_{L_2\epsilon_{|\mathcal{A}_t|}}(\bar{m}) \cap \mathcal{M}^{\text{RFC}}_t$, then any $\bar{m}^{\#}_{t,i} \in \mathbb{B}_{L_2\epsilon_{|\mathcal{A}_t|}}(\bar{m})$ will be optimal and $a^{\#}_{t,i}$ will be contained in $\kappa_t \circ \sigma_t^{\vec{d}_{t+1}}(\mathbb{B}_{L_2\epsilon_{|\mathcal{A}_t|}}(\bar{m}_t)) = \mathbb{B}_{\epsilon_{|\mathcal{A}_t|}}(\kappa_t \circ \sigma_t^{\vec{d}_{t+1}}(\bar{m}_t))$. It follows that the nearest neighbor approximation will have a maximum distance of $\epsilon_{|\mathcal{A}_t|}$ from $\kappa_t \circ \sigma_t^{\vec{d}_{t+1}}(\bar{m}_t)$. On the other hand, if $\left\{\bar{\kappa}^{\boldsymbol{d}_{t+1}}\right\}_{\boldsymbol{d}_{t+1}}$ are monotone, there exists such a simplex, and the linear approximation error over the simplex will also be bounded above by $\epsilon_{|\mathcal{A}_t|}$. Second, suppose $D_t > 1$ and there exist $N_{\bar{M}} + 1$ vertices of a simplex completely contained in $\bar{m}^{\#}_{t,i} \in \mathbb{B}_{L_2\epsilon_{|\mathcal{A}_t|}}(\bar{m}) \cap \mathcal{M}^{\text{RFC}}_t$. In this case, the distance between the exogenous grid points associated with the vertices of the simplex $\left\{a^{\#}_{t,0}, \ldots, a^{\#}_{t,i}, \ldots a^{\#}_{t,N_{\bar{M}}+1}\right\}$ and $\left\{\kappa_t \circ \sigma_t(\bar{m}^{\#}_{t,0}), \ldots, \kappa_t \circ \sigma_t(\bar{m}^{\#}_{t,i}), \ldots \kappa_t \circ \sigma_t(\bar{m}^{\#}_{t,N_{\bar{M}}+1})\right\}$ will be $C_0 L_2 L_1 \epsilon_{|\mathcal{A}_t|} + \epsilon_{|\mathcal{A}_t|}$. This gives us an upper-bound on the linear approximation error over the simplex of $C_0 L_2 \epsilon_{|\mathcal{A}_t|} + \epsilon_{|\mathcal{A}_t|}$. Third, suppose $D_t > 1$ and such a simplex does not exist. In this case, $\|\kappa_t(\sigma_t(\bar{m}^{\#}_{t,i})) - \kappa_t(a^{\#}_{t,i})\| < C_0 L_1 L_2 \epsilon_{|\mathcal{A}_t|} + \epsilon_{|\mathcal{A}_t|}$ for any $\bar{m}^{\#}_{t,i} \in \mathbb{B}_{L_2\epsilon_{|\mathcal{A}_t|}}(\bar{m})$. By the triangle inequality, the maximum error of a nearest neighbor approximation is $C_0 L_2 L_1 \epsilon_{|\mathcal{A}_t|} + 2\epsilon_{|\mathcal{A}_t|}$. □

References

Achdou, Y., Han, J., Lasry, J.-M., Lions, P.-L., and Moll, B. (2021). Income and wealth distribution in macroeconomics: A continuous-time approach. *Review of Economic Studies*, 89(1):45–86. 2, 6, 9

Aiyagari, S. (1994). Uninsured idiosyncratic risk and aggregate saving. *Quarterly Journal of Economics*, 109(3):659–684. 2, 6

Alfaro, I., Bloom, N., and Lin, X. (2024). The finance uncertainty multiplier. *Journal of Political Economy*, 132(2):577–615. 2

Arellano, C. (2008). Default risk and income fluctuations in emerging economies. *American Economic Review*, 98(3):690–712. 2

Arellano, C., Maliar, L., Maliar, S., and Tsyrennikov, V. (2016). Envelope condition method with an application to default risk models. *Journal of Economic Dynamics and Control*, 69:436–459. 2

Attanasio, O., Levell, P., Low, H., and Sanchez-Marcos, V. (2018). Aggregating elasticities: Intensive and extensive margins of women's labor supply. *Econometrica*, 86(6):2049–2082. 2

Auclert, A., Bardóczy, B., Rognlie, M., and Straub, L. (2021). Using the sequence-space Jacobian to solve and estimate heterogeneous-agent models. *Econometrica*, 89(5):2511–2547. 6

Bardoćzy, B. (2022). Spousal insurance and the amplification of business cycles. *Mimeo*. 6

Barillas, F. and Fernandez-Villaverde, J. (2007). A generalization of the endogenous grid method. *Journal of Economic Dynamics and Control*, 31(8):2698–2712. 5

Beraja, M. and Zorzi, N. (2023). On the size of stimulus checks: How much is too much? *Mimeo*. 2

Berger, D. and Vavra, J. (2015). Consumption dynamics during recessions. *Econometrica*, 83(1):101–154. 2, 4

Best, M. C., Cloyne, J. S., Ilzetzki, E., and Kleven, H. J. (2019). Estimating the elasticity of intertemporal substitution using mortgage notches. *Review of Economic Studies*, 87(2):656–690. 6

Bewley, T. F. (1972). Existence of equilibria in economies with infinitely many commodities. *Journal of Economic Theory*, 4(3). 11

Borovkov, A. A. (2013). *Stochastic recursive sequences*, pages 507–526. Springer London, London. 7

Brumm, J. and Scheidegger, S. (2017). Using adaptive sparse grids to solve high-dimensional dynamic models. *Econometrica*, 85(5):1575–1612. 2, 6

Buera, F. J. and Moll, B. (2015). Aggregate implications of a credit crunch: The importance of heterogeneity. *American Economic Journal. Macroeconomics*, 7(3):1–42. 2

Carroll, C. D. (1997). Buffer stock saving and the life-cycle/permanent income hypothesis. *Quarterly Journal of Economics*, 112(1):1–55. 2

Carroll, C. D. (2006). The method of endogenous gridpoints for solving dynamic stochastic optimization problems. *Economics Letters*, 91(3):312–320. 2, 3, 5, 9

Carroll, C. D. (2023). Theoretical foundations of buffer stock saving. *NBER Working Paper No. 10867*. 3, 10, 19, 23

Chan, T. C. Y., Mahmood, R., and Zhu, I. Y. (2023). Inverse optimization: Theory and applications. *Operations Research*, forthcoming. 3

Chen, L. and Xu, J.-c. (2004). Optimal Delauny triangulations. *Journal of Computational Mathematics*, 22(2):299–308. 11, 25

Clausen, A. and Strub, C. (2020). Reverse calculus and nested optimization. *Journal of Economic Theory*, 187. 9, 10, 22, 26

Cocco, J. F. (2005). Portfolio choice in the presence of housing. *Review of Financial Studies*, 18(2):535–567. 2

Coleman, W. J. (1990). Solving the stochastic growth model by policy-function iteration. *Journal of Business and Economic Statistics*, 8(1):27–29. 2, 9

Cooper, I. (2006). Asset pricing implications of nonconvex adjustment costs and irreversibility of investment. *Journal of Finance*, 61(1):139–170. 2

Crawford, R. and O'Dea, C. (2020). Household portfolios and financial preparedness for retirement. *Quantitative Economics*, 11(2):637–670. 6

Dávila, J., Hong, J. H., Krusell, P., and Ríos-Rull, J.-V. (2012). Constrained efficiency in the neoclassical growth model with uninsurable idiosyncratic shocks. *Econometrica*, 80(6):2431–2467. 2

Deaton, A. (1991). Saving and liquidity constraints. *Econometrica*, 59(5):1221. 2

Dechert, W. (1982). Lagrange multipliers in infinite horizon discrete time optimal control models. *Journal of Mathematical Economics*, 9:285–302. 11

Dobrescu, L., Motta, A., and Shanker, A. (2024a). The power of knowing a woman is in charge: Lessons from a randomized experiment. *Management Science*, forthcoming. 6

Dobrescu, L. and Shanker, A. (2023). Fast upper-envelope scan for discrete-continuous dynamic programming. *SSRN Working Paper No. 4181302*. 5, 6, 9, 20

Dobrescu, L. I., Fan, X., Bateman, H., Newell, B. R., and Ortmann, A. (2018). Retirement savings: A tale of decisions and defaults. *Economic Journal*, 128:1047–1094. 2, 28

Dobrescu, L. I., Shanker, A., Bateman, H., Newell, B. R., and Thorp, S. (2024b). Housing and pensions: Complements or substitutes in the portfolio allocation. *SSRN Working Paper No. 4069226*. 6, 10, 25

Druedahl, J. (2021). A guide on solving non-convex consumption-saving models. *Computational Economics*, 58:747–775. 5, 23, 25, 28

Druedahl, J. and Jørgensen, T. H. (2017). A general endogenous grid method for multi-dimensional models with non-convexities and constraints. *Journal of Economic Dynamics and Control*, 74:87–107. 3, 4, 5, 6, 7, 10, 11, 20, 21, 22, 23, 24, 25, 27

Duarte, V., Duarte, D., Fonseca, J., and Montecinos, A. (2020). Benchmarking machine-learning software and hardware for quantitative economics. *Journal of Economic Dynamics and Control*, 111:103796. 2

Fagereng, A., Gottlieb, C., and Guiso, L. (2017). Asset market participation and portfolio choice over the life-cycle. *Journal of Finance*, 72(2):705–750. 2

Fagereng, A., Holm, M. B., Moll, B., and Natvik, G. (2019). Saving behavior across the wealth distribution: The importance of capital gains. *NBER Working Paper No. 26588*. 2

Feinberg, E. A., Kasyanov, P. O., and Zadoianchuk, N. V. (2012). Average cost Markov decision processes with weakly continuous transition probabilities. *Mathematics of Operations Research*, 37(4):591–607. 14

Fella, G. (2014). A generalized endogenous grid method for non-smooth and non-concave problems. *Review of Economic Dynamics*, 17:329–344. 5, 6, 11, 13, 27

Fernández-Villaverde, J., Hurtado, S., and Nuño, G. (2023). Financial frictions and the wealth distribution. *Econometrica*, 91(3):869–901. 2

French, E. (2005). The effects of health, wealth, and wages on labour supply and retirement behaviour. *Review of Economic Studies*, 72(2):395–427. 2

González-Sánchez, D. and Hernández-Lerma, O. (2013). On the Euler equation approach to discrete–time nonstationary optimal control problems. *Journal of Dynamics and Games*, 1(1):57–78. 3

Gourinchas, P. O. and Parker, J. A. (2002). Consumption over the life cycle. *Econometrica*, 70(1):47–89. 2

Hai, R. and Heckman, J. (2019). A dynamic model of health, addiction, education, and wealth. University of Miami Business School Working Paper No. 2688384. 6

Hernandez-Lerma, O. and Lasserre, J. (2012). *Discrete-time Markov control processes: Basic optimality criteria*. Stochastic modelling and applied probability. Springer New York. 6, 7

Huggett, M. (1996). Wealth distribution in life-cycle economies. *Journal of Monetary Economics*, 38(3):469–494. 6

Hull, I. (2015). Approximate dynamic programming with post-decision states as a solution method for dynamic economic models. *Journal of Economic Dynamics and Control*, 55:57–70. 7

Iskhakov, F. (2015). Multidimensional endogenous gridpoint method: Solving triangular dynamic stochastic optimization problems without root-finding operations. *Economics Letters*, 135:72–76. 5, 9, 10

Iskhakov, F., Jørgensen, T. H., Rust, J., and Schjerning, B. (2017). The endogenous grid method for discrete-continuous dynamic choice models with (or without) taste shocks. *Quantitative Economics*, 8(2):317–365. 2, 5, 6, 11, 20, 27

Iskhakov, F. and Keane, M. (2021). Effects of taxes and safety net pensions on life-cycle labor supply, savings and human capital: The case of Australia. *Journal of Econometrics*, 223(2):401–432. 2

Iyengar, G. and Kang, W. (2005). Inverse conic programming with applications. *Operations Research Letters*, 33(3):319–330. 3, 9

Jang, Y. and Lee, S. (2023). A generalized endogenous grid method for default risk models. *SSRN Working Paper No. 3442070*. 2

Kaplan, G., Mitman, K., and Violante, G. L. (2020). The housing boom and bust: Model meets evidence. *Journal of Political Economy*, 128(9):3285–3345. 2, 4

Kaplan, G., Moll, B., and Violante, G. L. (2018). Monetary policy according to hank. *American Economic Review*, 108(3):697–743. 2

Kaplan, G. and Violante, G. L. (2014). A model of the consumption response to fiscal stimulus payments. *Econometrica*, 82(4):1199–1239. 2, 25, 27

Kekre, R. (2022). Unemployment insurance in macroeconomic stabilization. *Review of Economic Studies*, 90(5):2439–2480. 6

Khan, A. and Thomas, J. K. (2008). Idiosyncratic shocks and the role of nonconvexities in plant and aggregate investment dynamics. *Econometrica*, 76(2):395–436.

2

Krueger, D., Mitman, K., and Perri, F. (2016). Chapter 11 - Macroeconomics and household heterogeneity. In Taylor, J. B. and Uhlig, H., editors, *Handbook of Macroeconomics*, volume 2, pages 843–921. Elsevier. 2

Krusell, P. and Smith, A. A. (1998). Income and wealth heterogeneity in the macroeconomy. *Journal of Political Economy*, 106(5):867–896. 2, 6

Kumagai, S. (1980). An implicit function theorem: Comment. *Journal of Optimization Theory and Applications*, 31(2):285–288. 32

Laibson, D., Maxted, P., and Moll, B. (2021). Present bias amplifies the household balance-sheet channels of macroeconomic policy. *NBER Working Paper No. 29094*. 2

Lee, J. M. (2011). *Introduction to Topological Manifolds*. Graduate Texts in Mathematics. Springer, 1 edition. 14

Li, H. and Stachurski, J. (2014). Solving the income fluctuation problem with unbounded rewards. *Journal of Economic Dynamics and Control*, 45:353–365. 2, 5, 9, 10, 18

Ludwig, A. and Schön, M. (2018). Endogenous grids in higher dimensions: Delaunay interpolation and hybrid methods. *Computational Economics*, 51(3):463–492. 5, 25

Lujan, A. (2023). EGM^n: The sequential endogenous grid method. *Mimeo*. 5, 11

Ma, Q., Stachurski, J., and Toda, A. A. (2022). Unbounded dynamic programming via the Q-transform. *Journal of Mathematical Economics*, 100:102652. 5, 7, 10

Maliar, L. and Maliar, S. (2013). Envelope condition method versus endogenous grid method for solving dynamic programming problems. *Economics Letters*, 120(2):262–266. 2

Maliar, L., Maliar, S., and Winant, P. (2021). Deep learning for solving dynamic economic models. *Journal of Monetary Economics*, 122:76–101. 2, 6

Marimon, R. and Werner, J. (2021). The envelope theorem, Euler and Bellman equations, without differentiability. *Journal of Economic Theory*, 196:105309. 10

Pröhl, E. (2023). Existence and uniqueness of recursive equilibria with aggregate and idiosyncratic risk. *SSRN Working Paper No. 3250651*. 2

Reffett, K. L. (1996). Production-based asset pricing in monetary economies with transactions costs. *Economica*, 63(251):427–443. 2, 9

Rendahl, P. (2015). Inequality constraints and Euler equation-based solution methods. *Economic Journal*, 125(585):1110–1135. 3, 5, 10

Rincón-Zapatero, J. P. (2024). Existence and uniqueness ofsolutions to the Bellman equation in stochastic dynamic programming. *Theoretical Economics*, 19(3):184–197. 10

Rincón-Zapatero, J. P. and Santos, M. S. (2009). Differentiability of the value function without interiority assumptions. *Journal of Economic Theory*, 144(5):1948–1964. 3, 5, 9, 10, 12, 22

Rust, J. (1987). Optimal replacement of GMC bus engines: An empirical model of Harold Zurcher. *Econometrica*, 55(5):999–1033. 2

Sargent, T. J. and Stachurski, J. (2023). Completely abstract dynamic programming. *Working Paper No. 2308.02148*. 7

Sorger, G. (2015). *Dynamic economic analysis: Deterministic models in discrete time*. Thesis. Cambridge University Press. 5, 11

Stachurski, J. (2022). *Economic dynamics: Theory and computation (2nd edition)*. MIT Press. 5, 7

Wachsmuth, G. (2013). On licq and the uniqueness of lagrange multipliers. *Operations Research Letters*, 41(1):78–80. 31

White, M. (2015). The method of endogenous gridpoints in theory and practice. *Journal of Economic Dynamics and Control*, 60:26–41. 4, 5, 19, 20

Yogo, M. (2016). Portfolio choice in retirement: Health risk and the demand for annuities, housing, and risky assets. *Journal of Monetary Economics*, 80:17–34. 2, 25